

CHARACTERIZATION AND SPECTROSCOPY OF A SOLID-STATE SYNTHESIZED ER³⁺-DOPED CAYW PHOSPHOR FOR OPTOELECTRONICS

A thesis submitted

In partial Fulfilment of the
requirements for the degree of

MASTER OF SCIENCE

IN

PHYSICS

By

SWATIJA SAHOO

ROLL NO. (23/MSCPHY/49)

Under the Supervision of

Dr. Renuka Bokolia

&

Co-supervision of

Prof. A.S. Rao and

Dr. Shailesh Narain Sharma (Emeritus Professor)

Department of Applied Physics



DELHI TECHNOLOGICAL UNIVERSITY

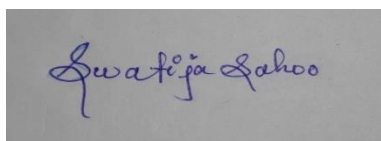
(Formerly Delhi College of Engineering) Bawana

Road, Delhi-110042, India June-2025

CANDIDATE'S DECLARATION

I hereby certify that the work, which is presented in the Dissertation-II entitled “**Structural and Spectroscopic Insights of Solid-State Synthesized Er^{3+} Doped CaYW Phosphor for Next-Generation Optoelectronic Applications**” in partial fulfillment of the requirements for the award of the Degree of Master of Science in Physics, submitted to the Department of Applied Physics, Delhi Technological University is an authentic record of our own work carried out during a period from June 2024 to May 2025, under the supervision of Prof. A.S Rao and Dr. Shailesh Narain Sharma.

The matter presented in the thesis has not been submitted for the award for any other course/degree of this or any other Institute/University.



Swatija Sahoo

(23/MSCPHY/49)

DELHI TECHNOLOGICAL UNIVERSITY

(Formerly Delhi College of Engineering)
Shahbad Daultapur, Main Bawana Road, Delhi-110042

CERTIFICATE

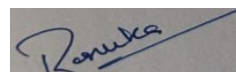
I certify that Ms. Swatija Sahoo (Enrollment No. 23/MSCPHY/49) has diligently performed all research work included in her thesis "**Structural and Spectroscopic Insights of Solid-State Synthesized Er³⁺ Doped CaYW Phosphor for next generation optoelectronic applications**" while under my supervision. This thesis constitutes the student asking for the degree of Master of Science from the Department of Applied Physics at Delhi Technological University, Delhi.

The thesis reflects Ms.Sahoo's independent and original effort. All experiments, analysis, and conclusions presented in this thesis were undertaken by her with excellent diligence and scholarly rigor. This research to the best of my knowledge is her original work and has not submitted, in full or in part, to support any claim for any other degree, diploma, or certificate at this or any other institution.

I am glad to be supervising her research project and appreciate her contributions to the growing understanding of phosphor material for next-generation optoelectronic applications.

Signature of Supervisor

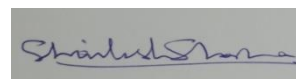
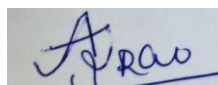
Dr. Renuka Bokolia



Assistant Professor
Department of Applied Physics
Delhi Technological University

Signatures of co-supervisors

Prof. A.S. Rao &
Dr. Shailesh Narain Sharma



Department of Applied Physics
Delhi Technological University, Delhi
Date : 09/06/2025

ABSTRACT

In this study, Calcium Yttrium Tungstate ($\text{Ca}_3\text{Y}_2\text{WO}_9$) (CaYW) phosphors doped with Er^{3+} ions were synthesized using the conventional solid-state reaction technique. An undoped host matrix CaYW was fabricated at three different temperatures—1100°C, 1200°C, and 1250°C—while varying the sintering duration between 10 and 12 hours. The prepared samples were further studied using the X-ray diffraction (XRD) technique, revealing that diffraction peaks of the sample sintered at 1100°C closely matched the standard JCPDS pattern (card number 00-038-0218). Furthermore, the material was identified as having a tetragonal crystal structure. Based on these findings, 1100°C was determined to be the optimal sintering temperature, with an ideal sintering time of 10 hours and 40 minutes. Following this, a series of $\text{CaYW}:\text{xEr}^{3+}$ phosphors was synthesized with varying Er^{3+} doping concentrations. The concentrations that were taken into calculations were 1 mol%, 3 mol%, 5 mol%, 7 mol% and 9 mol% of Er^{3+} . Their photoluminescence (PL) properties were examined along with the correlated colour temperature (CCT) and colour purity (CP), revealing strong luminescence in the green spectrum of the visible light region, with a peak centred at 563 nm when excited at 380 nm. However, concentration quenching was noted when Er^{3+} doping level exceeded 7 mol%. Consequently, 7 mol% was identified as the optimal doping concentration, and this sample was selected for further characterization techniques such as XRD, scanning electron microscope (SEM), ultra-violet (UV) spectroscopy along with diffuse reflectance spectra (DRS), fourier transformed infrared (FTIR) spectroscopy and thermogravimetric analyses (TGA) along with differential Thermal Analyses (DTA). Overall, the key insights of this research suggest that Er^{3+} -doped CaYW phosphors demonstrate promising potential for usage in white light-emitting diode (w-LED) applications.

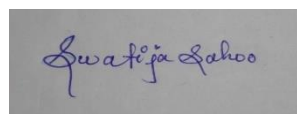
Keywords: phosphors, sintering, PL-quenching, chemical treatment

ACKNOWLEDGEMENTS

Our sincere gratitude goes out to Professor A.S. Rao & Dr. Shailesh Narain Sharma, Department of Applied Physics, Delhi Technological University, for all of their help, encouragement, and support during the writing of our master's thesis. His knowledge and wise counsel have greatly influenced the course and outcome of our study.

We especially want to thank Mrs. Bhawna for all of her help and support along the way.

Her perseverance and commitment have been invaluable in assisting us in overcoming the different obstacles this project has presented. We also want to express my sincere gratitude to National Physics Laboratory for helping to characterize our samples.. Throughout this journey, their confidence in us has been as a source of support and inspiration. Finally, we would want to express our gratitude to everyone who helped to successfully complete our thesis, whether directly or indirectly. Your assistance is much appreciated.



Swatiya Sahoo

(23/MSCPHY/49)

LIST OF RESEARCH WORK AND PUBLICATIONS

Title of the Paper (I): “Structural and Spectroscopic Insights of Solid-State Synthesized Er³⁺ Doped CaYW Phosphor for Next-Generation Optoelectronic Applications”

Author(s): Swatija Sahoo, A S Rao & Dr. Shailesh Narain Sharma

Name of Conference: 3rd International conference on “Advanced Function Material Devices for sustainable Development”(AFMD-2025)

Date and venue: March 5th-8nd (2025), Delhi Technological University.

Have you registered for the conference? **Yes**

Status of paper (Accepted/Published/Communicated):

Communicated in: Journal of electronics materials(JEMs)

Date of paper communication: 30th April, 2025

Date of paper acceptance: -----

TABLE OF CONTENTS

Title Page	(i)
Candidate's Declaration	(ii)
Certificate	(iii)
Abstract	(iv)
List of Research work and Publications	(v)
Contents	(vi)
List of tables and figures	(viii)
List of Abbreviations	(ix)

CHAPTER 1: INTRODUCTION

- 1.1 Phosphor
- 1.2 Host Matrix
- 1.3 Luminescent and its types
 - 1.3.1 Photoluminescence through Jablonski Diagram
- 1.4 Properties to consider for selecting host Material
- 1.5 Host Lattice
 - 1.5.1 Tungstate Host Lattice
- 1.6 Rare Earth

CHAPTER 2 : CHARACTERIZATION TECHNIQUES

- 2.1 X –Ray Diffraction
- 2.2 Scanning Electron Microscope
- 2.3 Fourier Transformed Infrared Spectroscopy
- 2.4 Diffuse Reflectance Spectra

2.5 Photoluminescence Spectroscopy

2.6 Time Resolved Fluorescence Spectroscopy

CHAPTER 3 : EXPERIMENTAL PROCEDURES

3.1 Synthesis of Samples

3.2 Characterization of samples

CHAPTER 4 : RESULTS AND DISCUSSIONS

\

4.1 Stuctural Analysis

4.1.1. XRD Analysis

4.2 Scanning Electron Microscope(SEM) analysis

4.3 Fourier Transformed Infrared Spectroscopy(FTIR)

4.4. DRS Results and analysis

4.5 Photoluminescence Studies

CHAPTER 5 :CONCLUSION

CHAPTER 6 : FUTURE SCOPE OF WORK

REFERENCES

CONFERENCE PARTICIPATION CERTIFICATION

PAPER SUBMISSION TO THE JOURNAL

PLAGIARISM REPORT

PROOF OF SCOPUS/SCIE/SCI INDEX

LIST OF FIGURES

- 1.1 Jablonski Diagram
- 1.2 White colour generation through red, green, blue
- 1.3 Periodic Table highlighting rare earth elements
- 2.1 Bragg's Law
- 2.2 Types of X-Ray Diffraction Methods
- 2.3 X-Ray diffraction methods
- 2.4 Scanning Electron Microscope
- 2.5 FTIR spectroscopy
- 2.7 Photoluminescence Spectrofluorometer
- 3.1 Programmable furnace
- 4.1 XRD plot for pure and optimized CaYW phosphors along with standard JCPDS
- 4.2 SEM images
- 4.3 FTIR graph for undoped(pure) and 7 mol% of Er^{3+} doped CaYW phosphors
- 4.4(a) DRS spectra of CaYW phosphors
- 4.4(b) Tauc's Plot
- 4.5(a) PL excitation spectra of CaYW phosphors
- 4.5(b) PL emission plot including 3-d plot
- 4.6 CIE diagram of CaYW
- 4.7 TGA and DTA plot for the host lattice

LIST OF ABBREVIATIONS

LED-Light-emitting diode

w-LED- White Light Emitting Diode

SSL-Solid State lighting

RRE - Rare Earth (Metals)

CCT- Correlated Colour Temperature

CRI- Colour rendering index

JCPDS- Joint Committee on Powder Diffraction Standards

XRD- X-ray Diffraction

SEM- Scanning Electron Microscope

FWHM- Full Width at Half Maximum

CIE-Commission International De L' Eclairage

UV - Ultraviolet

PL- Photoluminescence

CHAPTER 1: INTRODUCTION

1.1 Phosphor

Solid materials known as phosphors emit light when they are subjected to various forms of radiation such as electron beams, infrared, or ultraviolet light[1]. Phosphors exist in many different varieties, each possessing a distinct set of features such as the color of the light emitted and how long it lasts. The term "phosphors" has existed since the 17th century, which had been coined from an alchemist named Vincentinus Casciarolo in Italy, in the town of Bologna. He found a crystalline rock near a volcano that glowed red when it was placed in darkness after sunlight exposure. The rock, which came to be known as the "Bolognian stone," was subsequently found to be barite (BaSO_4)[2]. When it was fired, it was transformed into barium sulfide (BaS), which is now known to be a host material for phosphor compounds. This new discovery was followed by the finding of other such glowing rocks in various parts of Europe and they were all called phosphors—a name coined from the Greek word for "light bearer."

Phosphors usually consist of composite materials like oxides, oxynitrides, sulfides, selenides, halides, borates, and oxyhalides doped with very small quantities of activator ions[3]. Activator ions are transition metal elements or rare-earth elements that are the light emission centers. They possess discrete energy levels which are capable of getting excited or can engage in energy transfer and therefore emit light.

The energy absorption and emission phenomena have distinction which can be classified into two mechanisms: Up conversion and Down conversion [4]

Up conversion: In this mechanism the photons of lower frequencies like IR are converted into photons of higher frequencies usually in visible regions. This phenomenon is also known as anti-Stokes emission.

Down conversion: In this mechanism the photons of higher frequencies like UV or n-UV are converted into photons of lower frequencies usually in visible and IR region. This phenomenon is also known as Stokes emission .

A phosphor's efficiency is determined by its capacity to use excitation energy and emit light. To reduce afterglow, it is critical to reduce the duration between excitation and emission. The absorption of energy can occur at the activator ion or elsewhere in the lattice, but it must eventually be delivered to the radiating core before emission can occur. The absorbed energy can also be dispersed using radiation-free mechanisms, resulting in a loss in quantum efficiency. Effective phosphors retain their ions, reducing energy loss from non-radiative

transitions[5]. Contaminant ions can absorb or redirect energy, reducing the material's luminous qualities.

Phosphor materials are measured in terms of significant parameters such as emitting color range (e.g., red, green, and blue), luminescence equivalence, PL spectrum, quantum yield, and emission lifetime[6]. Color points are computed by dividing the emission spectrum energy according to the graphical Commission Internationale de l'Eclairage (CIE) rule. Luminosity count is large when the light is intense, and phosphors must therefore possess high lumen equivalence. A PL spectrum of electromagnetic radiation is formed on a transition of an atom or molecule from an upper to a lower energy level. The phosphors must possess a long emission life in order to be economical. Decay time, or afterglow or persistence, is the time taken by emission intensity to decrease to 10% of the original intensity upon the stoppage of stimulation. Decay time is a function of the intrinsic properties of the phosphor material [9]. Phosphor materials possesses enormous number of applications such as light emitting diode (LEDs), bio imaging, thermal sensors and other optical devices.

1.2 Host Matrix

Phosphors convert energy from sources of excitation, like X-rays and UV radiation, into visible light. Phosphorus can be categorized into three types :-

(a)Host luminophore: This type phosphors contain active centres itself which absorbs the incoming radiation and also emits the radiation. Inorganic hosts exhibit favourable characteristics such as being physically, thermally, and chemically inert, which makes them highly suitable choices. Nevertheless, self-activated hosts are more desirable than inorganic hosts due to their ability to generate powerful and wide- ranging visible radiation when exposed to UV light [7].

(b)Host + activator: In this type of phosphors they have a host matrix and an activator, which functions as the emitting centre. In this category the host are inactive but having luminescent active centres. The activator utilizes the intrinsic radiation to amplify the emission intensity[8].

(c)Host + sensitizer + activator: Phosphors of this category has a sensitizer which absorbs the incoming radiation, then the transfer of energy happens from sensitizer to activator in the host. Due to sensitizer there is an enhancement in the luminescent properties of the materials.

1.3 Luminescence and its type

After the discovery of phosphors in 17th century every researcher were starting to do research to find various methods for luminescence and the reason behind them. Luminescence is a phenomenon of emission of radiation from a material not from heat[9]. The material absorbs the incident radiation and re-emit the radiation in different wavelength resulting in luminescence. Excitation process in phosphor can occur due to various methods like electricity, heat, mechanical force, chemical reaction etc[10].

Luminescence can be seen on are day to day life like in lamps, television or smart phone screens etc[11].

Depending on different causes of excitation, the processes of luminescence can be divided into different types:-

(a)Photoluminescence : In photoluminescence the excitation of electrons happens when electromagnetic radiations incident the surface of the phosphor. It can beclassified into two different types depending upon the process – Phosphorescence andFluorescence.

(b)Chemoluminescence : In chemoluminescence light is emitted as a result of chemical reaction. There is no heat interaction present in this reaction and it does not require any external light, it is self-sustaining in the chemical system. Production of light is just a result of electronic transition in the molecules involved in chemical reaction. Fireflies are a typical example of living organisms showing chemiluminescence. A chemical reaction between luciferin and oxygen is analysed by an enzyme luciferase to yield release of light. Luminol is a chemiluminescent substance employed in forensic examination to identify blood at the scene of crime.

(c) Bioluminescence : It is a type of luminescence which arises from living organisms through chemical reactions. It can be seen in various organisms like in bacteria, fungi, insects and deep see fishes.

(d)Thermoluminescence : Thermoluminescence TL is the phenomenon in which some materials after being irradiated with ionizing radiation emit light when heated. It is commonly used in the fields of archaeology and earth science to date artifacts and rocks, and in some radiological methods to determine radiation exposure. The basic idea is – some mineral absorb energy of ionizing radiation slowly, and they return the absorberd energy with light when we heat them.

(e)Electroluminescence : In this method the luminescence occurs by the action of electric field on the phosphor. Like in LEDs the electron hole pair recombination results in the luminescence. When the luminescence occurs due to free electrons then it is called cathodoluminescence.

(f)Radioluminescence : Radioluminescence is a condition where some materials emit visible light when bombarded by ionizing radiation. This phenomenon is separate from that of thermoluminescence, which is the process in which a material gives off light upon heating after having been exposed to ionizing radiation. Radioluminescence is the emission of light from environmental chemicals, the direct interactions with ionizing radiation.

1.3.1 Photoluminescence through Jablonski Diagram :

Photoluminescence is when a material absorbs photon (particle of light) and then send out light. It is observed in material that is illuminated at a particular wavelength, causing it to emit light at a higher wavelength. In essence, the material absorbs energy from photons

and gives it back in the form of light. Photoluminescent is generally divided into two major type: phosphorescence and fluorescence. Jablonski diagram can explain these very easily.

Phosphorescence: Phosphorescence is the process by which substances continue to produce energy and glow even after the radiation source has been shut off. This glow gradually diminishes in brightness over a period of milliseconds to days[10]. This phenomenon can arise when two excited states with different total spin exhibit similar energy levels. The ground state and one of the excited states are shown in the graphic as singlets ($S=0$), while the following excited state is shown as a triplet ($S=1$)[12]. Although spectroscopic transitions between singlet and triplet levels are forbidden by the rule $\Delta S=0$, there is no constraint if the excited states are transferred kinetically, that is, through radiationless transitions produced by collisions[13]. Transfer between the two potential curves can only happen around the cross-over point. The molecule cannot return to the excited singlet state once it enters the triplet state and begins to lose vibrational energy. As a result, it will eventually arrive at the triplet state's level of zero velocity ($\dot{v}=0$). Despite being technically forbidden by spectroscopic constraints, a transition from the present state to the ground state can nonetheless happen, albeit much more slowly than an electronic transition that is permitted[10]. Phosphorescent materials have the ability to emit radiation for a prolonged period of time, ranging from seconds to minutes or even hours, after they have absorbed energy. The phosphorescence spectrum typically comprises of frequencies that are lower than those absorbed[12].

Fluorescence : Fluorescence is the process in which substances generate energy promptly and cease glowing when the stimulating radiation is deactivated. The phenomenon can be elucidated by a diagram, where the molecule, following electronic excitation, is in a highly vibrational state. In this state, any surplus vibrational energy can be dissipated through intermolecular collisions. The conversion of vibrational energy into kinetic energy in the sample results in the generation of heat. This movement of energy across different levels without the emission of radiation is known as "radiationless"[10, 14]. Once the excited molecule transitions to a lower vibrational state, it releases radiation and returns to its ground state. This emitted radiation, known as the fluorescence spectrum, typically has a lower frequency than the absorbed radiation. However, in certain circumstances, it can have a higher frequency. The duration from when the substance is first absorbed to when it returns to its original state is extremely brief, approximately on a scale of 10^{-8} seconds[10].

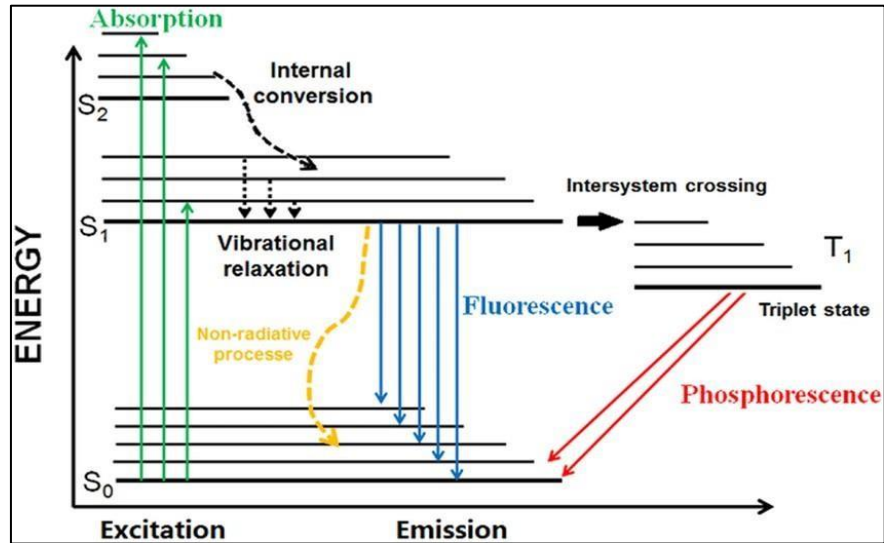


Figure 1.1 Jablonki Diagram

White Light Emitting Diodes (w-LEDs)

LEDs become one of the key technological developments of modernity in their delivery of environmentally conscious and cost-effective artificial light. White light-emitting diodes (w-LEDs) have recently been developed as solid-state lighting (SSL) sources. They offer benefits including energy efficiency, reliability, high output, long life, high efficiency and environmental protection[15, 16].

Significant study has been conducted on luminous materials doped with rare earth (RE) due to recent improvements in SSL technologies[17]. A significant proportion of industrial energy is allocated to lighting, underscoring the importance of energy-efficient and eco-friendly solutions. SSL, which utilizes LEDs with p-n junctions, fulfils these requirements by offering advantages such as high luminous efficacy, low power dissipation, durability, and extended operational lifespan. Presently, w-LEDs predominantly utilize blue-emitting diodes with a wavelength range of 450-470 nm to stimulate YAG:Ce phosphors, resulting in the emission of yellow light. However, this approach does not include the red component, resulting in a low Colour Rendering Index (CRI) and a high Correlated Colour Temperature (CCT). Another option is to utilize an n-UV LED chip combined with RGB phosphors, although ensuring the accurate colour ratio can be difficult and expensive.

To address these problems, it is economically more feasible to use doping with a single rare earth ion, e.g. Er^{3+} possesses emission bands in the green and blue wavelength ranges. Erbium-doped phosphors emit white light with enhanced quantum efficiency, thermal stability, cost-effectiveness, and necessary CIE and CCT values. There are three significant ways to produce white light with LEDs: blue LEDs with YAG:Ce phosphor, n-UV LEDs with RGB phosphors, and single-phase component phosphor utilized with UV

or n-UV LEDs. The latter one is of increasing interest due to its reliability, efficiency, low energy requirement, and eco-friendliness in production. The advancement of w-LED applications relies heavily on the advancements in the development of co-doped RE on single-phase phosphors[18]. The current research is geared towards enhancing luminescence performance with charge compensation and ion replacement techniques.

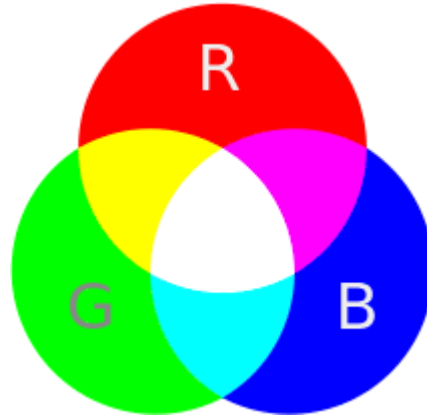


Fig 1.2: White Colour generation through Red, Green and Blue

1.4 Properties to consider for selecting host material.

CCT: A light source's colour appearance can be measured using the Correlated Colour Temperature (CCT). It compares the colour of the light to that of a reference source when heated to a specified temperature, which is measured in degree Kelvin (K). The CCT of a light is a general indication of its visual appearance, and in particular how warm or cool it appears. Opposite to the temperature scale, light sources of a lower CCT below 3200 K are usually considered "warm", whereas those with a CCT above 4000 K are usually considered cool.

CRI: Color rendering index (CRI) refers to the capacity of a light source to accurately replicate the colors [19, 20] of different objects when compared to an ideal or natural light source. A reference source, such as daylight, is characterized by a Color Rendering Index (CRI) value of 100. A CRI (Color Rendering Index) of 100 indicates the highest level of faithfulness to a reference, while a CRI below 0 indicates the lowest level of faithfulness.

Luminous efficacy: The term "luminous efficaciousness" describes a light source's ability to transform a certain kind of energy into light. It is measured in lumens per watt (lm/W), which is the ratio of the total luminous flux emitted by the light source to the electricity consumed.

Luminous efficiency: Luminous efficacy can be standardized by dividing it by the highest achievable luminous efficacy, resulting in a dimensionless measure [21] known as luminous

efficiency. The definition states that the highest achievable luminous efficacy is equivalent to a luminous efficiency of 100%.

Quantum efficiency: The quantum efficiency of a phosphor material is the precise measurement of the proportion of emitted photons to absorbed photons[22]. The term "quantum yield" is another name for it.

1.5 Host Lattice

To select a host some of the properties are observed to have best host for respective applications. The properties are :

- (a) For optical applications, it is crucial to have a host lattice with low phonon energy and excellent chemical and temperature stability.
- (b) The host lattice must possess a wide energy bandgap and excellent optical transparency in both the visible and ultraviolet spectra.
- (c) Within 4f energy levels the optical transitions of dopant ions are significantly influenced by the host lattice materials. For example, the crystal field produced by the host lattice can remove the requirement for selecting particles with the same parity and alter the likelihood of f-f transitions[17, 23].
- (d) Host materials with low lattice phonon energies are desirable because they exhibit little non-radiative loss and high radiative emission[24].

1.5.1 Tungstate host lattice : Tungstate is the standard inorganic luminescent material. CaWO_4 is a naturally emitting material and has Scheelite type structure[24]. Tungstate Tungstate compounds glow on their own from differences in the vibration state of W^{6+} ions which are surrounded by four Oxygen atoms in a tetrahedron[25, 26]. The latter complexes have the character of good chemical and thermal stability.

Trivalent rare earth (RE) ions have identical ionic size and chemical characteristics, making their inorganic compounds excellent host materials for RE dopant ions. Furthermore, alkaline earth ions such as calcium (Ca^{2+}), strontium (Sr^{2+}), and barium (Ba^{2+}), as well as certain transition metal ions like zirconium (Zr^{4+}) and titanium (Ti^{4+}), also display a similar ionic size to rare earth (RE) ions. Consequently, host materials often utilize inorganic substances that contain these ions.

1.6 Rare Earth ions

The advances and enhancements of phosphors has enabled the realization of luminescent materials with rare earth (RE) elements used as luminescent centres or activators in several host lattices. While RE elements are undoubtedly expensive, their ability to produce specific spectrum distributions makes them commercial viable due to their very useful abilities[27, 28]. The commercial opportunities for luminescent materials (doped with RE), has slowly been growing mainly due to their feasible high quantum efficiency, demonstrated stability, and application areas.

RE (rare earth) elements are a cluster of 17 elements that consists of 15 lanthanides (La with

atomic number 57 to Lu atomic number 71) plus Sc and Y with atomic numbers (21 and 39). The RE set of elements are abundant, however they are seldom obtained in compact and economically viable options. The lanthanide elements (Ce³⁺ to Lu³⁺) also possess partially occupied 4f orbitals, thus resulting in different of luminescent behaviours for each ions energy level[29, 30]. Luminescent ions can be dopants inside a vast array of host phosphor lattices.

RE ions are important in display technology because they exhibit outstanding luminescent properties, which are expressed as unique peak emission bands. They are used for the detection of radiation and light in solid-state materials. For the phosphor products to be used in industry, they should have high efficiency of luminescence, unmatched chemical and thermal stability, long usable life, and environmental sustainability. It is through appropriate doping with rare earth (RE) elements that these properties achieve these attributes; this has been an active area of technological research.

Rare earth doped phosphors can be simply classified into two groups with regard to their spectral or emission properties: broad band emitting phosphors (Eu²⁺, Tb³⁺, Gd³⁺, Yb³⁺, Dy³⁺, Ce³⁺) or narrow band emitting phosphors (Sm³⁺, Tm³⁺, Er³⁺, Nd³⁺) . The 5d-4f transitions in ions like Eu²⁺ and Ce³⁺ are very sensitive to local changes in structure and provide broad band emission. However, the effect of local atomic arrangements affects very few of the 4f levels. The dominant nearby atomic arrangements produce constant and stable emission spectra of unique attributes, due to shielding effects[8].

In conclusion, rare earth ions continually play a regulatory role in the development of high-performance luminescent materials, especially in the realms of solid-state lighting (SSL) and display technologies. In relation to this work, rare earth ions have particular electronic configurations and transitions which serve as the basis for building effective, durable and versatile light sources[27, 28].

H	Rare Earth Elements																He	
Li	Be											B	C	N	O	F	Ne	
Na	Mg											Al	Si	P	S	Cl	Ar	
K	Ca	Sc	Ti	V	Cr	Mn	Fe	Co	Ni	Cu	Zn	Ga	Ge	As	Se	Br	Kr	
Rb	Sr	Y	Zr	Nb	Mo	Tc	Ru	Rh	Pd	Ag	Cd	In	Sn	Sb	Te	I	Xe	
Cs	Ba	*	Hf	Ta	W	Re	Os	Ir	Pt	Au	Hg	Tl	Pb	Bi	Po	At	Rn	
Fr	Ra	**	Rf	Db	Sg	Bh	Hs	Mt	Ds	Rg	Cn	Uut	Fl	Uup	Lv	Uus	Uuo	
		*	La	Ce	Pr	Nd	Pm	Sm	Eu	Gd	Tb	Dy	Ho	Er	Tm	Yb	Lu	
		**	Ac	Th	Pa	U	Np	Pu	Am	Cm	Bk	Cf	Es	Fm	Md	No	Lr	
			Light Rare Earth Element								Heavy Rare Earth Element							

Fig 1.3: Periodic table highlighting Rare earth elements

CHAPTER 2 : CHARACTERIZATION TECHNIQUES

2.1 X-RAY DIFFRACTION

X-ray diffraction is a readily used technique which can be used to determine crystal structure, phase purity, crystallite size, distance between crystal planes, lattice parameter, and stresses in materials. This technique was developed by German Physicist Von Laue in 1912, but English Physicists W. H. Bragg and W.L. Bragg were the first to successfully use XRD[31, 32] to determine the crystal structures of the various crystals. X-Rays are electromagnetic waves of a very short wavelength of about a few angstroms (10^{-10})[31]. They were discovered by German Physicist Roentgen in 1895.

Diffraction of light is a well-known phenomenon of optics. The deflection of light through an obstacle or through an aperture is called diffraction. Light diffraction does not take place unless the obstacle has a rudiment situated in relationship to the wavelength, which under most conditions causes the corners of the obstacle to act like secondary sources for the light and that there is a phase relationship between each wave leaving these secondary sources. The only requirement is diffraction to take place is that the width of the obstacle must be lower than or of the same order as the wavelength of the wave. For a similar setting, the crystal lattice can diffract the x-rays because the inter-planar spacing (d) are of comparable values when compared to the wavelength of the x-rays. The phase difference generated due to the atomic planes are given by the relation

$$2d \sin \theta = n\lambda \quad (2.1)$$

This equation is known as Bragg's law [31, 33, 34]

Here, d refers to inter planar distance, λ is the wavelength of the X-ray used and θ is called Bragg's angle.

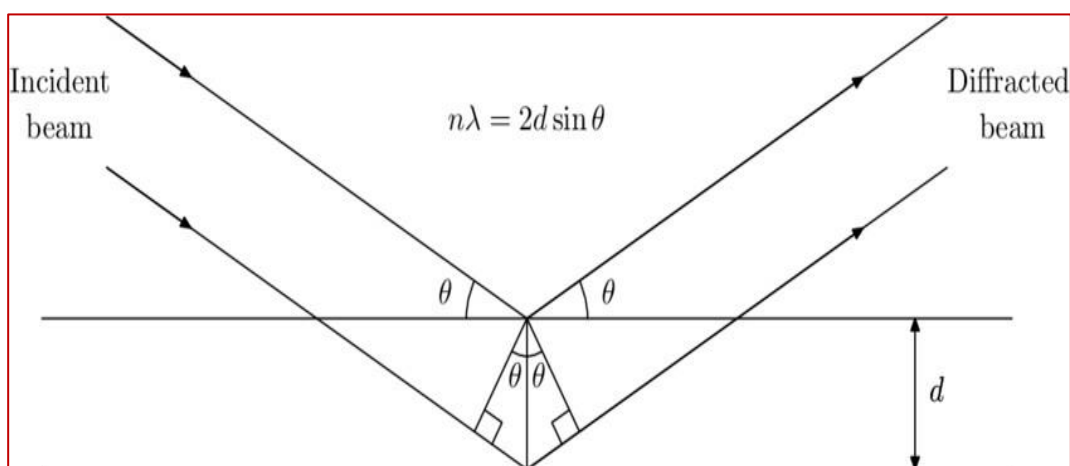


Fig. 2.1. Bragg's law

The X rays falling on the sample and gets diffracted in all direction, and detected by a detector that can be either movable or fixed. On the basis of geometry of the experiment there are three types of XRD methods:

1. Laue's Method
2. Rotating Crystal Method
3. Debye-Scherrer Method (Powder crystal Method) [31, 35]

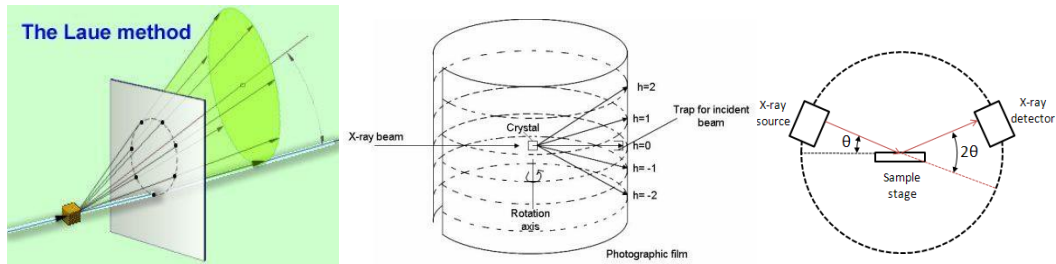


Fig. 2.2. Types of X-ray diffraction methods

The Powder crystal method is usually used, this sample is in powdered form. The intensity of the diffracted beams is then collected at different diffraction angles (θ) using the detector. The position of the intensity of the diffracted beam at different positions of θ depends on crystal structure and alignment of the atomic planes within the crystal sample. The obtained spectrum is then compared with standard available databases heaps provided by the Joint Committee on Powder Diffraction Standards (JCPDS)[35, 36]. This spectrum is used for determining the crystal structure and other parameters.

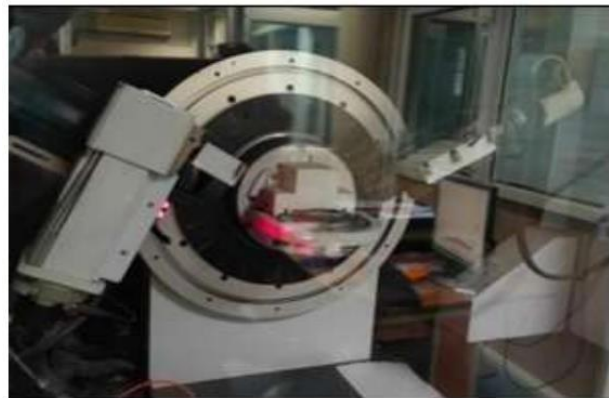


Fig. 2.3. X-Ray Diffractometer

2.2 Scanning Electron Microscope

Electron microscopes use a beam of electrons instead of light to look at very small scales.

Electron microscopes have a higher magnification and better resolution than optical microscopes. They have an electron source, magnetic lenses [37] that focus the electron beam, and detectors to collect the signals[38, 39]. Scanning electron microscopy is used to show the morphology of the sample. An electron beam is focused on a small area of the sample, that transfers energy in that area and removes electrons from the surface of the sample called secondary electrons. The primary electrons that are struck the surface of the sample and reflected are called backscattered electrons. At time x-rays are also given off due to the interaction between the electron source and the sample. Unique signal types give different types of information about the sample. To get a complete SEM image of the specimen, the electron beam is moved across the entire area of the specimen, and the signals obtained from the surface of the specimen are transformed into images, that show the morphology and composition of the surface.

The X-rays generated by the sample are used to analyze the elemental composition and concentration of elements in the sample, this analysis is done by energy dispersive spectrometer (EDS)[37]

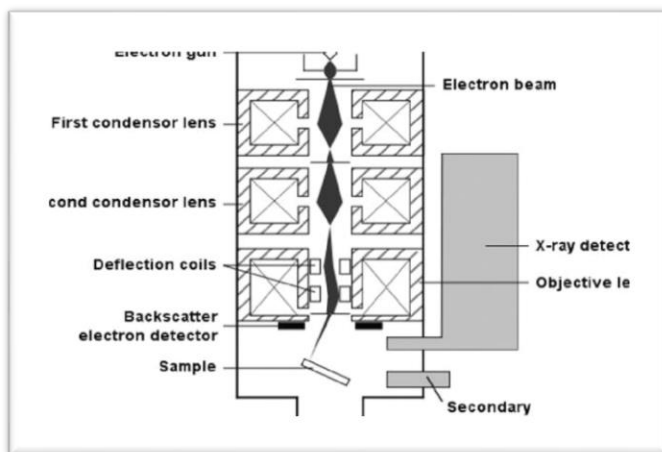


Fig. 2.4. Scanning Electron Microscope

2.3 Fourier Transformed Infrared Spectroscopy

The infrared (IR) region of the electromagnetic spectrum can be used to excite the vibration levels of the polar molecules[40, 41]. The sample is irradiated with IR in the range 400-4000 cm^{-1} , which excites the polar groups present in the decomposition products and changes the energy levels causing stretching and bending vibrations of bonded polar molecules in general.

Altogether in stretching vibration, there is a change in bond length between two atoms while in bending vibration the atoms change the angle with the bond length changing[42]. The absorbance or transmittance data for the sample are plotted against energy range to obtain a FTIR spectrum and different energy bands appearance on the FTIR spectrum can help in the identification of the different functional groups present in the sample[43].

FTIR analysis can also be used to determine the potential to find the OH content in the sample, which is mostly aimed to be low in case of the phosphors; as this can absorb the excitation energy and this would be lowered phosphor efficiency.

The FTIR spectrometer works on the basis of a Michelson interferometer, where a beam splitter splits the beam into two parts, and then the distance two mirror beams travel work at right angles, one of the mirrors travels and the other mirror is stationary positioned[41, 44]. The resultant reflectance that comes from these mirrors create a interferogram which passes through the sample and then to a detector which detects the photons of which wavelength is absorbed or transmitted.

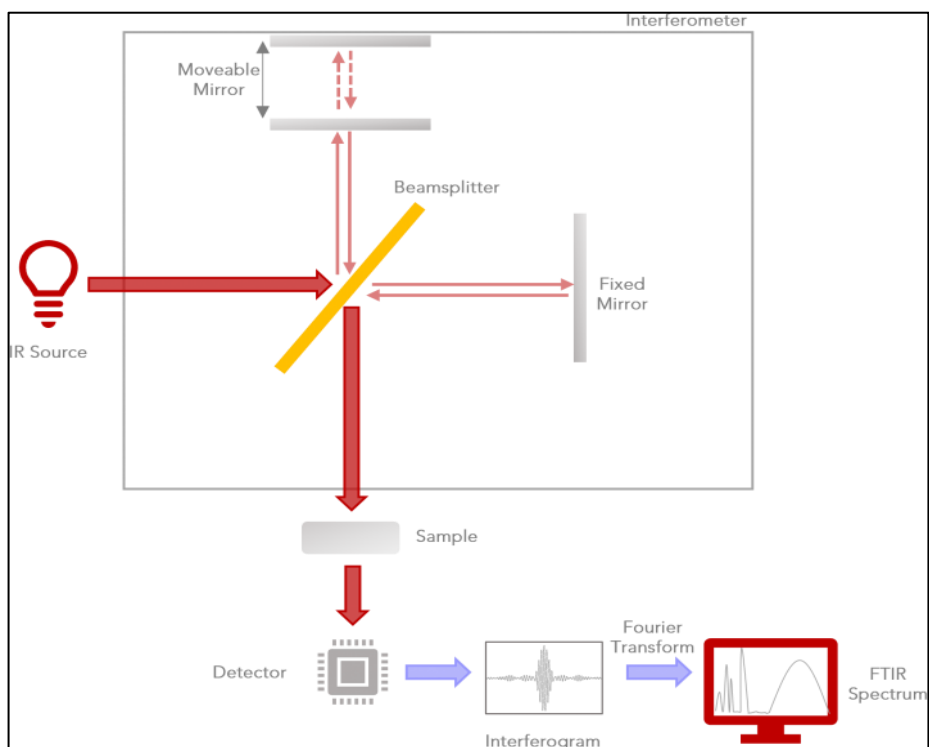


Fig. 2.5. FT-IR Spectroscopy

2.4 Diffuse Reflectance spectra

Diffused reflectance spectroscopy is a type of absorption spectroscopy performed in the UV-visible range of the electromagnetic spectrum; it can be used to find the electronic energy levels as well as the optical energy band gap. In DRS, the light reflected from the sample is detected rather than the light transmitted through the sample. Generally UV-Visible spectroscopy is performed on a sample [45] dispersed in a suitable liquid, however if the particle size is not small enough for it not to precipitate in solution it becomes difficult to evaluate the absorption spectrum because it may not be clear what fraction of the light absorbed was as a result of the original particle size retention in solution, as opposed to a sample aggregation occurring that prevents the wavelength from acting on the original size of the particle. To overcome this complication the DRS spectrum can be taken instead of the UV-Vis spectrum of a powdered sample. (Kubelka and Munk proposed this theory for use of the DRS, ref for UV-VIS formula paper).

The optical energy band gap is calculated from DRS curve using the formula[45–47]

$$[F(R_{\infty})h\nu]^n = (h\nu - E_g) \quad (2.2)$$

Where, $h\nu$ represents the energy of a photon of frequency ν , E_g the optical energy bandgap, and $F(R_{\infty})$ the Kubelka-Munk function ($R_{\infty} = R_{\text{sample}}/R_{\text{standard}}$). Here, C is proportionality constant and $n = 1/2$ or 2 for indirect or direct band gaps, respectively. The Kubelka-Munk

(K-M) function can be obtained using the following equation

In this equation, the sample's reflectance, molar absorption coefficient, and scattering coefficient are represented by the variables R , k , and s , respectively[48, 49].

2.5 Photoluminescence Spectroscopy (PL)

When light strikes the sample, the photon associated with the incident light is absorbed and the electrons become excited and move to higher energy (excited states). This process is called photo- excitation, and when the electrons come back down to their original stable states they cause the sample to glow or yield photo-luminescence (PL)[50, 51]. Note that the emitted energies can either be greater or lower than the excitation energies.

Phosphors can be categorized based on energy conversion into two main categories, either up converting where the emitted energy is greater than that of the excitation energy and down converting where the emitted energy is lower than the excitation energy[52–54]. There are two types of spectra are produced in PL spectroscopy, the PL excitation spectrum which gives details about the excitation wavelengths for photo-excitation and the PL emission spectrum showing the emission ranges of the sample[51, 54].

The rare earth ions doped phosphors generally have their excitation in the UV or near UV range and their emission is in the entire visible range[55]. A PL spectrometer is made up of a light source that emits light with multiple wavelengths, a monochromator to select a specific wavelength, sample holder and a detector to collect the emitted spectrum of light transmitted through the sample[56, 57]. The monochromator utilize a diffraction grating for wavelength selection.

The sample holder has a cuvette made of a material paving way for wavelengths employed. The detector has a photomultiplier tube to amplify signals and recording spectra[57]. The intensity of the applicable wavelength of light has been made. The intensity of the peaks in the spectra will be as it is from the transitions from different energy levels. The spectra of samples having different doping concentrations can be sampled one at a time, and the intensity variation of a specific peak in the different sample may divulge to the levels of energy transfer processes that may be engaged. If there is any sensitizer present in the sample that absorbs the excitation energy and transfers that energy to the luminescent active centre of the sample.

Photoluminescence excitation and emission spectra of phosphor were investigated using a Jasco 8300 FP Spectro fluorophotometer based on breath Xenon lamp[58].



Fig.2.7. Photoluminescence Spectro fluorophotometer

2.6 Time Resolved Fluorescence Spectroscopy

This is an important spectroscopy, which provides information about the lifetimes of unfavourable states, probabilities and efficiencies of energy transfer process from a donor ion to an acceptor ion [59]. A short pulse is used for excitation of the sample where the time could be kept as short as possible (shorter than the decay time)[60]. Emission is measured with intensity and time to obtain fluorescent decay curves and then the life time is calculated by doing exponential fitting of the curves[61].

CHAPTER 3 : EXPERIMENTAL PROCEDURES

3.1 Synthesis of Sample

Er^{3+} ions doped phosphors with molar composition (mol%) $(3\text{CaCO}_3) - [(1-x) \text{Y}_2\text{O}_3] - (\text{WO}_3) - (x\text{-Er}_2\text{O}_3)$ is prepared through the traditional solid-state method. The starting chemicals that were used are CaCO_3 (100.0869 g/mol), Y_2O_3 (225.81 g/mol), WO_3 (231.84 g/mol), Er_2O_3 (382.56 g/mol) obtained in high-quality high powdered form. The erbium doping was introduced at the yttrium site. All the required pre-requisite reactants were taken in the proper stoichiometric measurement ratio were uniformly blended with the help of an agate mortar, with acetone acting as a diluting agent. The homogeneous powder mixture was transferred into an alumina crucible and then annealed in a furnace at temperatures varying from 600°C to 1100°C for about 10 to 12 hours to facilitate the required chemical reactions. The temperature was gradually raised from room temperature to the annealing temperature, and then cooled down subsequently to room temperature at a maintained rate of $5^\circ\text{C}/\text{min}$. The powder thus heated is crushed again to get a fine and homogenous mass for instrumental study. The sample so prepared is then undergone through XRD analyses. The result so obtained from XRD for our host (CaYW) matched with the standard JCPDS file (card number 00-038-0218) which confirms our host is fit for further synthesis. The host material was doped with Er^{3+} in successively higher concentrations varying from 1 mol% to 9 mol%. The different concentrated samples underwent same steps of synthesis as the pure host.

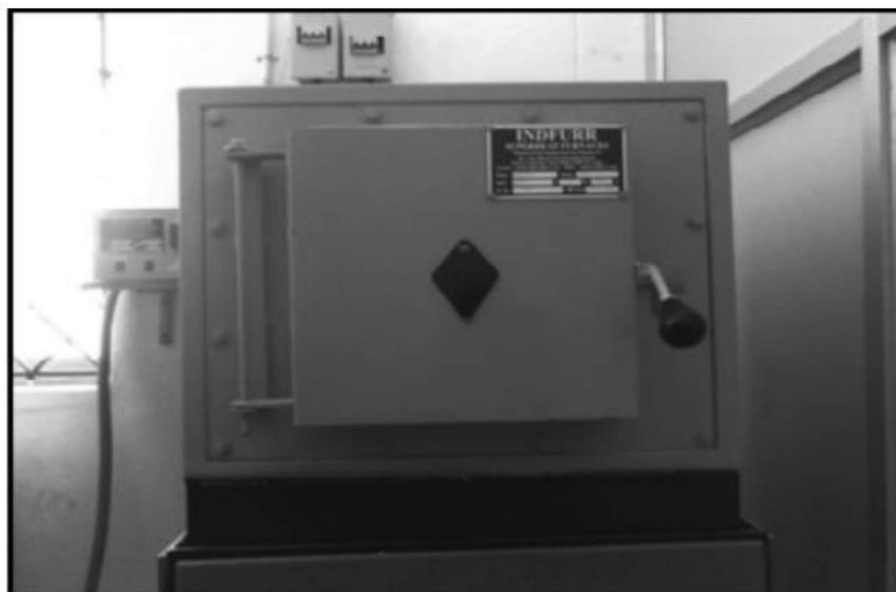


Fig. 3.1 Programmable Furnace

3.2 Characterization of samples

The structural aspects and phase purity of the synthesized CaYW phosphor were characterized thoroughly via X-ray diffraction (XRD) studies. XRD measurements were conducted using a Bruker D-8 Advance diffractometer, a standard tool for high-precision structural studies of crystalline materials. The instrument was operated at an accelerating voltage of 40 kV and current of 40 mA using Cu-K α radiation as the X-ray source. XRD data was collected from a range of $20^\circ \leq 2\theta < 60^\circ$. This is sufficient to capture the major diffraction peaks corresponding to the crystallographic planes of the phosphor phase. All diffraction patterns obtained from the study will provide evidence for the formation of the intended crystalline phase and indicate that there are no secondary or impurity phases confirming phase purity of the synthesized material.

The optical properties of the CaYW phosphor were also explored in addition to structural characteristics. Ultraviolet-visible-near infrared (UV-Vis-NIR) absorbance spectra were obtained from a range of 200 nm to 1500 nm using a Jasco V-770 spectrophotometer. This extended range of measurements allowed us to examine fundamental absorption characteristics of our phosphor, as well as electronic transitions taking place inside the sample which would provide additional knowledge regarding the bandgap and electronic structure of the material.

In addition, the photoluminescence (PL) properties are important for determining the potential of the phosphor in light-emitting applications. Both excitation and emission spectra were measured using a Jasco FP-8300 fluorescence spectrophotometer with a xenon lamp. The xenon lamp is useful because it provides a broad excitation range that is stable across the UV-visible range, providing an opportunity to correctly observe the luminescent response. The drawn measurement can provide insight into activator ion energy levels and wavelengths of emission and the luminescence efficiency and intensity thereby contributing to the assessment of the phosphor for use in photonic optoelectronic or display technologies.

CHAPTER 4: RESULTS AND DISCUSSION

4.1 Structural Analysis

4.1.1 XRD analysis

An X-ray Diffraction (XRD) examination was performed to determine the crystal structure and phase purity of CaYW/x:Er³⁺ phosphors. XRD provides important information about crystallographic structure, which allows us to conclude whether any structural changes occurred as a result of dopant incorporation. The XRD patterns were collected on undoped (pure) CaYW and Er³⁺doped (optimized) CaYW samples and were compared with the standard reference pattern with the Joint Committee on Powder Diffraction Standards (JCPDS) card number 00-038-0218.

The experimental patterns recorded, and all the diffraction peaks collected exhibited good correspondence with standard JCPDS data for the phase. The strong correlation of these patterns indicated that our material synthesized the intended phase with less effect on the crystal structure than expected. The diffraction pattern indicates that this material crystallized in a tetragonal crystal structure and corresponding space group of I4₁/a, which is consistent with the expected structure of the CaYW host lattice for a phosphor.

No additional peaks or movement of peak position was observed upon Er³⁺ doping, which suggests that the dopant ions entered the host lattice without disturb the lattice structure. As a result, we can conclude that the host material is structurally stable, and we successfully substituted Er³⁺ ions into the host lattice without forming a secondary phase, also verifying that CaYW is a suitable host matrix for rare-earth doping in luminescence.

The site preference of dopant ions was analysed through ionic radius difference calculations (ΔR) using the relation [62]

$$\Delta R = \frac{R_H - R_A}{R_H} \times 100 \% \quad (4.1)$$

where, R_A and R_H corresponds to the ionic radii of the activator and host cations, respectively. The calculated ΔR values of 21.57% (for Y³⁺ /Er³⁺) confirm preferential substitution at yttrium sites, as values below 30% indicate favourable incorporation [63].

Miller indices were assigned to all diffraction peaks by matching with standard reference data. The tetragonal crystal system was further verified through interplanar spacing calculations using Bragg's law ($2d_{hkl}\sin\theta_{hkl} = \lambda$) and the tetragonal structural relation [62]

$$\frac{1}{d^2} = \frac{h^2 + k^2}{a^2} + \frac{1}{c^2} \quad (4.2)$$

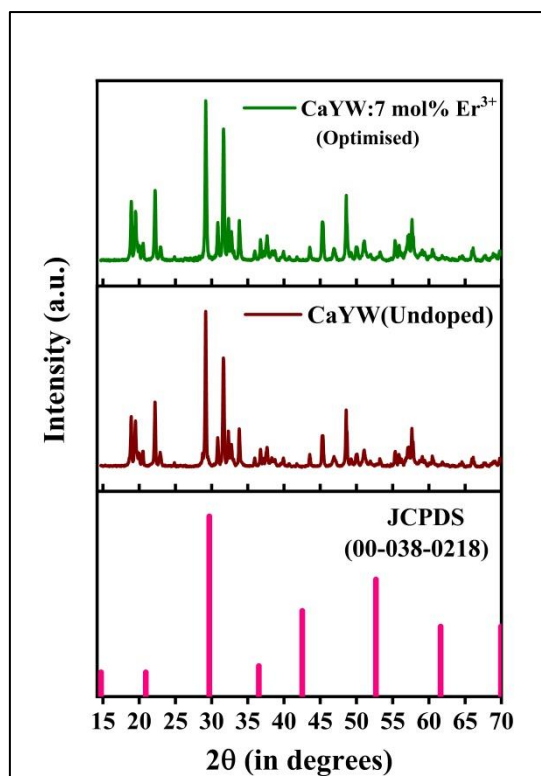


Fig 4.1. XRD plot for pure and optimised CaYW along with standard JCPDS.

Lattice parameters were determined by initially identifying (h k l) planes to calculate the a-axis, followed by using other reflections to determine the c-axis. The calculated parameters closely match standard values. This indicates an optimal doping threshold near 7 mol% for maintaining crystalline integrity in this system.

4.2 SEM analysis

Scanning electron microscope (SEM) characterization was applied to investigate the particulate characteristics of prepared phosphors. Microstructural development of undoped and Er^{3+} -doped CaYW samples with different dopant content ranging from 1 to 9 mol% has been illustrated in **Figure 4.2**. The micrographs reflect irregular spherical particles that exhibit varied extents of agglomeration due to high-energy mechanical processing and calcination at high temperatures used during synthesis.

A perceptible change in particle size has been noted with higher concentrations of Er^{3+} . The mean sizes of particles at the lower doping concentrations were observed to rise, and higher concentrations seemed to yield a fall. This is a result of the dual function of Er^{3+} doping substitution of Y^{3+} sites with Er^{3+} at moderate concentration levels enhances inter-particle electrostatic attractive forces owing to the higher electronegativity of the dopant, thus promoting coalescence of the particles. At high doping levels, however, interstitial occupation of Er^{3+} ions will hamper the crystalline field and lower particle attraction and hence the particle size decreases.

spectra is that samples show similar infrared absorption bands irrespective of Er^{3+} concentration. The stability of the peaks in their positions suggests that the doping of Er^{3+} ions has little to no effect on the structural characteristics of the host lattice, maintaining the symmetry of crystal structure.

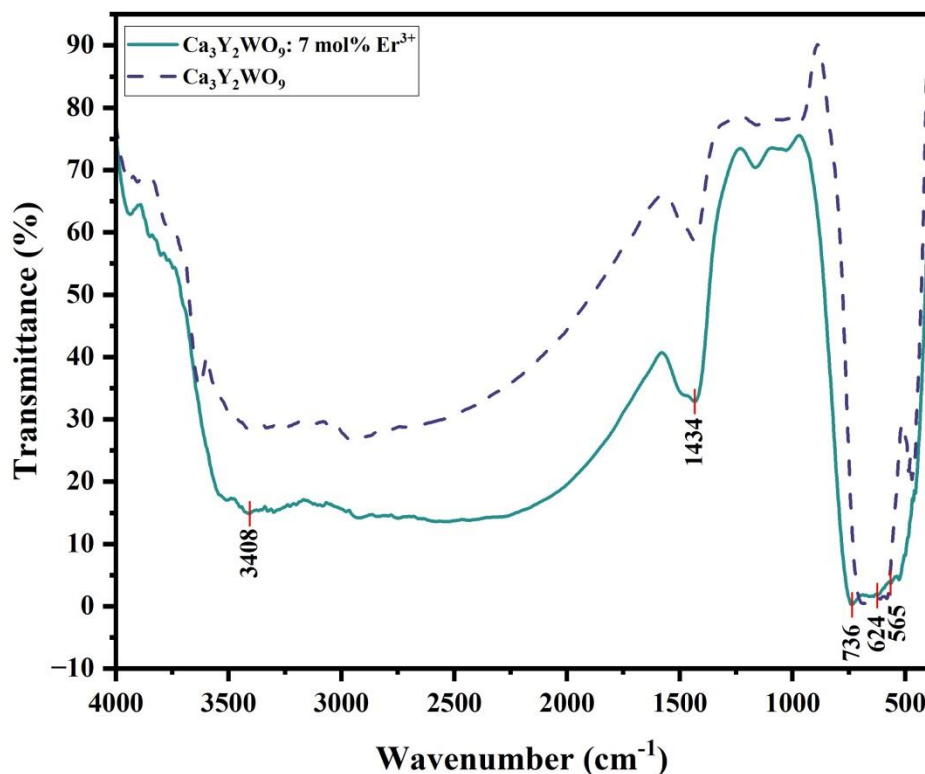


Fig 4.3. FTIR graph for undoped (pure) and 7 mol % Er^{3+} doped CaYW phosphors.

Two dominating well-defined absorption energy band in the spectrum are seen at 565 and 736 cm^{-1} which are indicating about the asymmetric modes of stretching of Ca–O bonds and to the bridging vibrations of the O–Ca–O bonds, respectively [64, 65]. These features, therefore, affirm the formation of the CaYW compound with a well-defined crystalline phase.

In addition, minor vibration bands are observable at 1434 cm^{-1} . The bending vibration of the C–H bonds is likely responsible for the absorption observed in 1434 cm^{-1} , coming from residual organic substances or environmental contamination[66, 67]. The O–H stretching vibration is usually obtained within the range ($3000\text{--}3500\text{ cm}^{-1}$), which suggests a surface hydroxyl group. For our host material, the O–H vibration is obtained at 3408 cm^{-1} . Fourier transform infrared (FTIR) analyses strongly emphasises on the fact that the synthesized luminescent-phosphor maintains a pure, uni-phase calcioscheelite-type and morphologically tetragonal-like structure without any detectable secondary phases or structural distortions due to Er^{3+} doping. Maintaining this structural integrity will impart the desired stability and performance of this material in optoelectronic applications.

4.4 Diffuse reflectance spectra(DRS) results and analysis

The optical band gap serves as a fundamental parameter in evaluating a material's potential as an efficient host. Materials exhibiting band gaps between 3 to 5 eV are particularly desirable for luminescent applications due to their optimal energy absorption and emission characteristics. Diffuse reflectance spectra(DRS) was employed to examine the optical reflectance characteristics and estimate the band gap of synthesized phosphors. **Figure 4.4(a)** shows the diffuse reflectance spectra DRS spectra of $\text{CaYW}:x \text{Er}^{3+}$ where, $x = 3, 5, 7, 9$ doped (CaYW) phosphors over a large wavelength range of 200–800 nm. An intense reflectance peak at 278 nm assigns to the charge transfer band (CTB) resulting from electronic transitions between the oxygen 2p orbitals and the tungsten 5d orbitals ($\text{O}^{2-} \rightarrow \text{W}^{6+}$). The Plumb intensity of this band which exists for each sample indicates that reflectance due to the host lattice is not affected by Er^{3+} doping. In contrast, several reflection peaks attributed to Er^{3+} ion transitions are seen to level up with the increment in dopant concentration because higher concentrations of Er^{3+} cations will reflect more photons, hence displaying characteristic reflection bands more strongly.

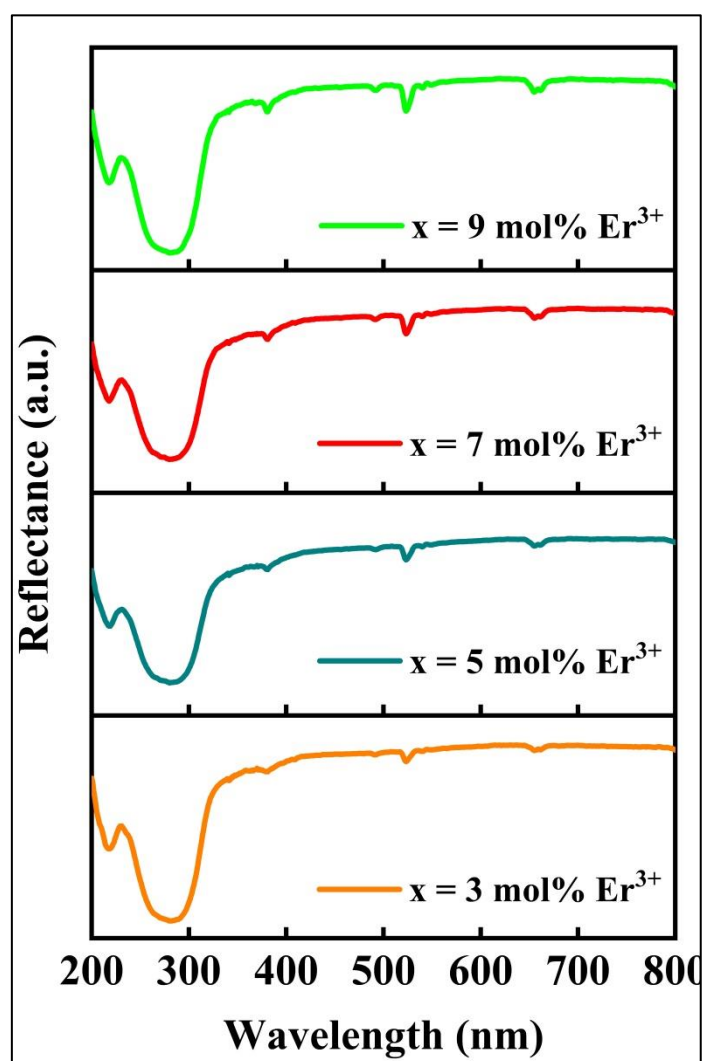


Fig 4.4(a) DRS spectra of 3, 5, 7, 9 mol% Er³⁺ doped CaYW phosphors.

A calculation of the value of the optical energy band gap (E_g) is done by applying the application of the Kubelka-Munk (K-M) function on the diffuse reflectance data. The K-M equation connects reflectance (R_∞) to scattering coefficient (S) and absorbance coefficient (K) through the expression [68, 69]:

$$F(R_\infty) = \frac{(1-R_\infty)^2}{2R_\infty} = \frac{K}{S} \quad (4.3)$$

where $F(R_\infty)$ represents the K-M function and R_∞ represents the sample's reflectance relative to a BaSO₄ reference.

The absorption coefficients were correlated to the photon energy through the Tauc's relation [62, 69]:

$$\alpha h\nu = C(h\nu - E_g)^{m/2} \quad (4.4)$$

where, C is the constant of proportionality, $h\nu$ represents the energy incident, and m is a constant associated with various electronic transitions that is taking place. In direct band gap semiconductors like CaYW, for $m = 1$ some transitions are allowed. Assuming the scattering coefficient is wavelength-independent and constant, the K-M equation simplifies into

$$[f(R_\infty)h\nu]^2 = C_1(h\nu - E_g) \quad (4.5)$$

Here C_1 is another constant. The values of the band gaps were calculated by the extrapolation of the linear portion of the $[F(R_\infty)h\nu]^2$ against the energy plot to the point at which $[F(R_\infty)h\nu]^2$ equals zero. Thus, the Kubelka-Munk plots for pure CaYW and CaYW:x mol% Er³⁺ where x=1, 3, 5, 7, 9 mol % Er³⁺ are presented in **Figure 4.4(b)**, respectively indicating band gap energies of 3.94 eV, 3.93 eV, 3.92 eV, 3.89 eV, 3.88 eV, 3.85 eV.. The nearly same band gap value for 1 mol% and 3 mol% doped samples can be attributed to a very minor difference in concentration of the activator ion.

The optical band gap of a material decreases with increasing doping concentration due to the increased bonding (or interactions in the case of other break bonds) between dopant atoms and the host lattice which leads to band tailing and localized states near the band edges.

However, there are cases, especially at higher doping densities, that the band gap anomalously increases (typically ~ 0.1 eV). These anomalous increases in band gap are most commonly attributed to the Burstein-Moss (B-M) Effect. The B-M Effect occurs where the doping concentration is so high that the carrier density of the material has increased (specifically in the conduction band) such that occupied states in the conduction band occupy the lowest energy states, which requires an increase in energy levels occupied by the valence band electrons to overcome the band gap. The observed energy gap appears larger because it

now requires more energy to bridge the gap as the lower energy states are occupied with carriers [70]. The observed increase in energy gap is not from a real change in the electronic structure of the material, rather the state filling that is a result of the high carrier concentration due to the added dopant atoms, and the change in available electronic transitions.

Therefore, valence electrons need photons of higher energy to move to the conduction band . The widening of the band gap was noted to finalise the successful integration of Er^{3+} ions into the CaYW lattice at higher concentrations.

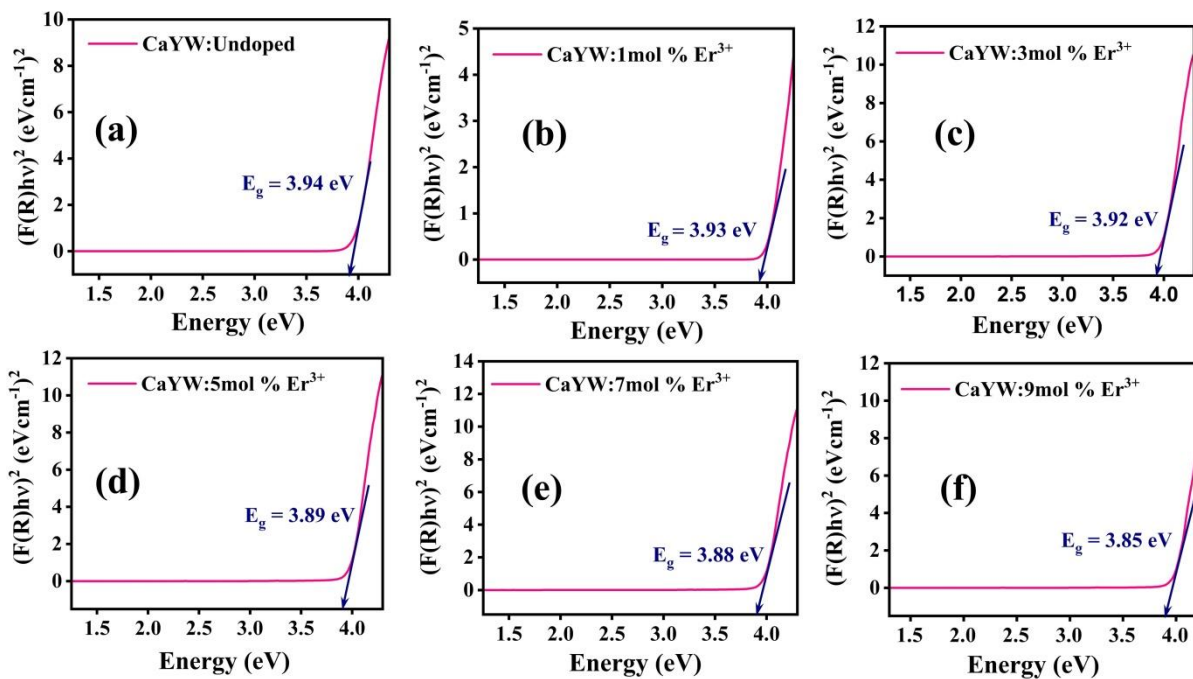


Fig 4.4(b). (a)- (f) represents Tauc's plots for undoped CaYW and $\text{CaYW}:\text{xEr}^{3+}$ (where $\text{x}=1, 3, 5, 7, 9$ mol%) phosphors.

4.5 Photoluminescence Studies (PL)

Photoluminescence (PL) is an important optical property of phosphor materials and has seen widespread research interest owing to their uses in one way or another in lighting, display technologies, and optoelectronic devices. It is defined as the light emission from a material subsequent to the absorption of photons, and generally involves electronic transitions from excited states back to lower energy states. It is important in the determination of material properties and is extensively used in the fields of semiconductors, optoelectronics, and bio-imaging [71, 72]. In phosphor materials, activator ions—typically rare-earth or transition metal ions— participate in luminescence by introducing discrete energy levels in the band gap of the

host lattice. The photoluminescence and specific wavelength emission experienced is usually a function of several factors; the host matrix, activator doping concentration, and synthesis conditions. Photoluminescence characterization allows an accurate understanding of phosphor materials PL behavior and gives valuable insight into their electronic structure and is an important step to help maximize its performance in real world applications.

Rare earth ions have very interesting photoluminescence(PL) properties by virtue of their unique 4f electronic transitions, resulting in sharp emission peaks, high colour purity, and long luminescence lifetimes [72, 73]. The compounds exhibit multimodal emission behaviours such as up conversion (UC), downshifting (DS), and quantum cutting (QC) [71]. Rare earth-doped PL materials find applications in several areas including spectral conversion technologies for enhancing the efficiency of silicon solar cells, lighting and display devices based on Eu^{3+} -doped phosphors for red emission in LEDs, and sensing technology using luminescent metal-organic frameworks (MOFs) for the targeted identification of ions of the elements belonging to the rare earth group[72–74]. The PL processes of rare earth elemental systems normally go through energy transfer mechanisms where sensitizers such as Yb^{3+} , which absorb photons and transfer energy to activators like Ho^{3+} or Tm^{3+} [71, 74]. These unique properties make rare earth photoluminescent materials integral in advanced applications in optoelectronics, energy harvesting, and biomedical technology [72, 74].

The excitation spectra were recorded while maintaining a constant emission wavelength at 563 nm in the excitation range width (300 nm-500 nm). The excitation spectra presented in **Figure4.5(a)** display several distinct peaks at 366 nm, 385 nm, 410 nm and 490 nm, each of which is likely due to common f-f orbital transitions of Er^{3+} ions [75]. Notably, the maximum excitation occurs at 380 nm, and this suggests that the phosphor material is optimum in its excitation efficiency in terms of being excited by commercially available near-ultra-violet(UV) excitation light sources. The property renders the material perfectly suitable for real applications in which near- ultra-violet (UV) excitation is employed. The peaks of excitation confirm the presence of Er^{3+} ions within the host matrix to be effective and preserving common rare-earth optical features.

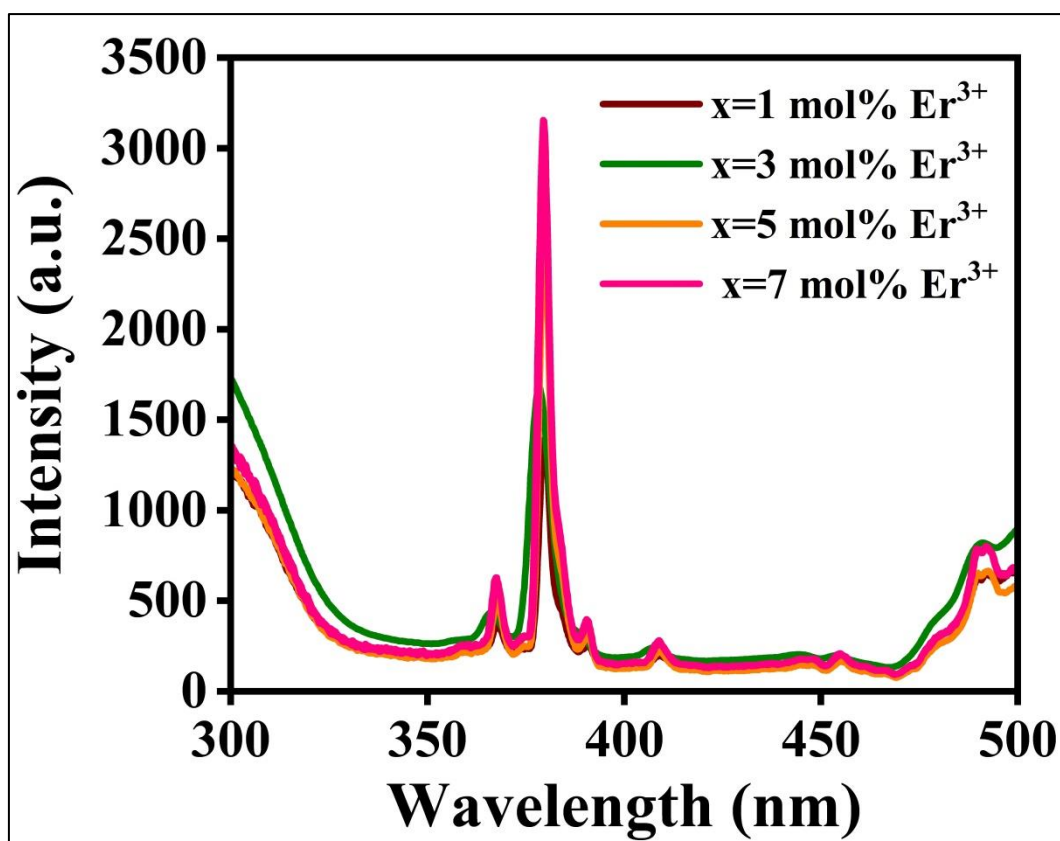


Fig 4.5(a) PL excitation spectra of CaYW:x mol% Er³⁺ phosphors.

Emission spectra of CaYW:x mol % of Er³⁺ excited at 380 nm within the range (500 nm-600 nm) are shown in **Figure 4.5 (a)**. Two intense peaks at 532 and 563 nm are present in the spectra. These peaks refer to the electronic transitions of erbium ions: from ²H_{11/2} to ⁴I_{15/2}, from ⁴F_{9/2} to ⁴I_{15/2} [75, 76]. **Figure 4.5(b)** represents the 3D plot of photoluminescence(PL) properties of Er³⁺ doped CaYW phosphor.

The phosphor's luminescence is dependent on the concentration of activator ions. There will be a weaker emission intensity with a lower concentration of activators since there are fewer light-emitting centres. Conversely, too great an excess of activators also causes a diminution of intensity through a phenomenon called concentration quenching. This happens because energy transfer among neighbouring activator ions becomes excessively efficient, which results in the energy dissipation through non-radiative processes, decreasing the total emission. Therefore, for the maximum emission intensity, optimal activator ion concentration must be achieved.

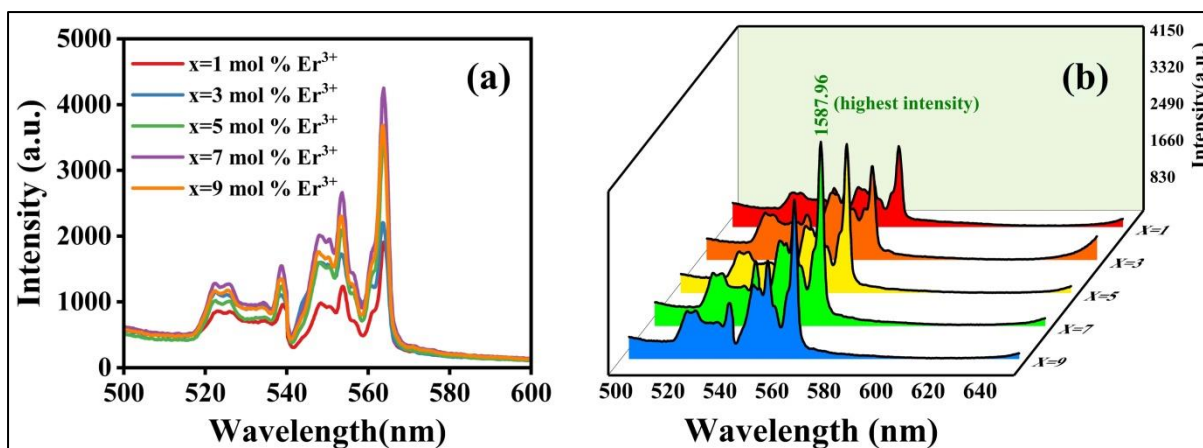


Fig4.5(b). (a) represents the PL emission plot for various molar concentrations of Er doped CaYW phosphors and (b) represents the 3D PL emission plot for various molar concentrations of Er³⁺ doped CaYW phosphors.

With the increment in doping concentration of Er³⁺, the shape of the emission spectra remains unchanged but the intensity rises until a 7 mol% doping concentration since more luminescent sites are formed. With further concentrations above this, however, the intensity begins to fall because of the concentration-quenching effect.

4.6 Photometric Results

The photometric characterization of photoluminescence (PL) in phosphor materials is important to consider whenever a new phosphor material is evaluated for lighting and display applications, where colour quality and colour consistency are significant factors. The correlated colour temperature (CCT) is one of the quantities arising from photometric analysis and reflects the 'colour' of the emitted light. The CIE1931 colour space is typically referenced to obtain the chromaticity coordinates of the photoluminescent emission, which in turn is used to calculate the CCT. Mccamy's empirical relationship provides a convenient way to estimate CCT based on the chromaticity coordinates of the photoluminescence emission [77].

Mccamy's relationship can be useful in instances of photoluminescent emissions when one only has chromaticity coordinates and needs a quick approximation of the CCT, as it can simplify the complex calculations associated with the Planckian locus, provided through a reasonably straight-forward mathematical equation. Equation 1, which calculates the distance from a specific location in the CIE diagram to the blackbody locus, estimates the CCT using a reasonable approximation of the chromaticities nearest the Planckian locus.

The development of various types of white light-emitting phosphors with different levels of warmth and coolness can highlight the importance of directly relating the CCT to the Mccamy relationships; therefore the CCT and Mccamy relationships are key components in the further development and optimisation of new phosphor materials.

Photometric investigation plays an essential role for deeply analysing characteristics and the quality of light emitted. This analyses involves evaluating key parameters such as colour coordinates (x, y) followed by Correlated Colour Temperature (CCT) along with Colour Purity (CP) of the emitted light by synthesized phosphor materials. The CIE chromaticity diagram for CaYW:xEr³⁺ phosphors derived from PL emission plot is shown in **Figure 4.6**, which indicates green emissions in the wavelength range of approximately 520–550 nm. Notably, this emission exhibit minimal spectral shift at 7 mol % Er³⁺ concentration, which is associated with the characteristic 4f orbital transitions of electrons of Er³⁺ ions. The correlated colour temperature(CCT) of a phosphor corresponds to the temperature of ideal black body that emits light with similar chromaticity. It is calculated using McCamy's empirical relation [77]:

$$CCT = -437n^3 + 3526n^2 - 6823n + 5520.23 \quad (4.6)$$

where $n = (x - x_e) / (y - y_e)$, and $x_e = 0.332$ and $y_e = 0.185$ representing the chromaticity epicentre. The study reveals that all CaYW: xEr³⁺ samples have correlated colour temperature (CCT) values nearly exceeding 5000 K, indicating their suitability for cold white light applications [62]. Colour purity(CP) is a measure of the saturation of emitted light and is calculated using the formula: [76]

$$CP = \frac{\sqrt{(x-x_i)^2 + (y-y_i)^2}}{\sqrt{(x_d-x_i)^2 + (y_d-y_i)^2}} \times 100\% \quad (4.7)$$

Here, $(x_i, y_i) = (0.311, 0.343)$ represents the equal-energy white point, while (x_d, y_d) denotes the dominant wavelength coordinates [28]. The optimised sample exhibit colour purity (CP) value above 90%, reflecting high colour saturation and suitability for display applications. The derived values for colour coordinates are x:0.343, y:0.642 and correlated colour temperature(CCT) is estimated to be approximately 6710.43 with a colour purity (CP)of 92.7%. The high correlated colour temperature (CCT >5000 K) and CP (>90%) value suggest that CaYW: xEr³⁺ phosphors are promising candidates for use as green-emitting materials in cold white light emitting diodes(LEDs). These phosphors demonstrate excellent optical properties, including efficient luminescence and high thermal stability, making them suitable for advanced display applications and solid-state lighting.

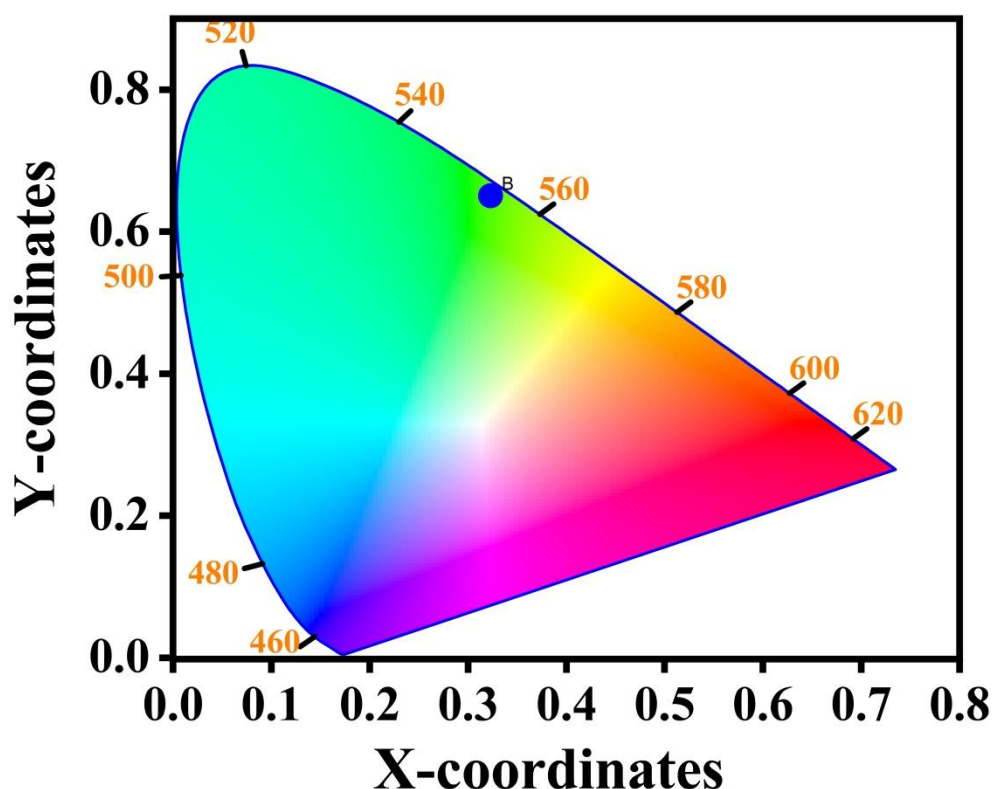


Fig 4.6. CIE diagram of CaYW: 7 mol% Er (optimised)

4.7 TGA results and analysis

Thermogravimetric analysis (TGA) is a useful analytical method for investigating the thermal and compositional properties of phosphor materials, including those using tungstate hosts. In TGA, you measure the mass change of your sample against changing temperature or time in a controlled atmosphere (typically either air or an inert gas). For phosphorescent materials, such as the tungstates here, TGA can identify decomposition behavior, moisture content, and possibly phase transitions in these compositions. Tungstates have strong-metal oxygen bonds that are maintained by the geometry of the phosphor lattice meaning that the material is expected to show memory of its high temperature stability.

A typical TGA curve for a tungstate chloride phosphor would likely show a small weight loss before 200 °C, from the loss of physically adsorbed water or residual organics part of the synthesis process. It would also potentially show thermal memory or an underlying thermal stability given little-to-no weight loss over a longer, higher temperature range. Tungstate phosphors can be subjected to higher temperatures in the thermally steady-state temperature evaluation method for LED applications or display backlighting. The doping of phosphors may alter or influence their thermal response, either as a result of the interactions with and additional phase of the dopant, or potentially due to an alteration of the dynamics of the lattice. All of which can be examined using TGA analysis.

Thermogravimetric analyses (TGA) was used to study the thermal stability and decomposition behaviour of the as-prepared undoped $\text{Ca}_3\text{Y}_2\text{WO}_9$ host lattice in the temperature range of 28–1000°C. The thermogravimetric analyses (TGA) curve in **Figure 4.7** shows two different stages of weight loss. The first stage, between 200–600°C, shows a mass loss of 4.21%, which can be due to the removal of adsorbed moisture or partial decomposition of residual carbonates. The second phase, recorded at 600–800°C, exhibits a larger weight loss of 12.69%, attributed to the volatilisation of oxides and extensive structural rearrangement. Beyond 800°C, there is no mass loss detected, which indicates that the calcination process is complete and that there is the production of a stable, single-phase $\text{Ca}_3\text{Y}_2\text{WO}_9$ host lattice.

Complementary Differential Thermal Analyses (DTA) also clarifies the thermal transitions in phosphor formation. An endothermic peak at 778°C corresponds to the mass loss region in the thermogravimetric analyses (TGA) curve, indicating a phase transformation resulting in the thermally stable $\text{Ca}_3\text{Y}_2\text{WO}_9$ structure[78–84].

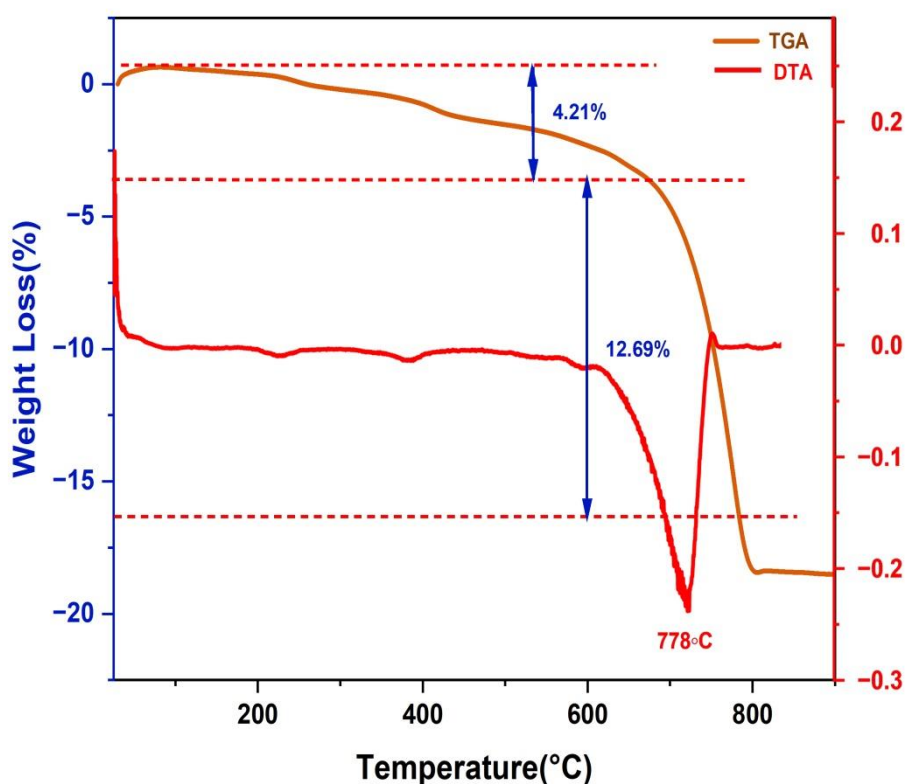


Fig 4.7. TGA and DTA curves for $\text{Ca}_3\text{Y}_2\text{WO}_9$ host lattice

CHAPTER 5 : CONCLUSION

The synthesis and characterization of Erbium (Er^{3+})-doped Calcium Yttrium Tungstate ($\text{Ca}_3\text{Y}_2\text{WO}_9$) phosphors for optoelectronic applications, especially LEDs, were performed. The phosphors were synthesized via a traditional high-temperature solid-state reaction method. Optimal sintering conditions sample was determined to be at 1100°C for 10 hr and 40 min, to achieve well-crystallized tetragonal structure. The X-ray diffraction (XRD) patterns confirmed phase purity and crystallinity, as they corresponded to the standard patterns of $\text{Ca}_3\text{Y}_2\text{WO}_9$ and demonstrated, the incorporation of Er^{3+} ions to the host lattice without any secondary phases.

The photoluminescence studies demonstrated a distinctly emission green peak at 563 nm when the excitation wavelength was at 380 nm. This was associated with the transition levels $4\text{S}_{3/2} \rightarrow 4\text{I}_{15/2}$ of the Er^{3+} nuclei. It was also established that a doping concentration of 7 mol% was the best doping concentration, and that concentrations above 7 mol% exhibited deactivation concentration quenching effects, therefore emission green intensity was diminished.

Thermogravimetric analysis (TGA) was conducted to confirm the thermal stability of the phosphors, $\text{Ca}_3\text{Y}_2\text{WO}_9:\text{Er}^{3+}$ which indicates that they are able to withstand high-temperature development suitable for device applications. Photometric results demonstrate a high correlated color temperature ($\text{CCT} > 5000\text{ K}$) which may support the cool white-light characteristic of the sample, along with good color purity ($> 90\%$) the materials exhibit potential towards the development of cold white light LED technologies. A trichromatic green LED prototype was developed using a near-ultraviolet (UV) chip combined with $\text{Ca}_3\text{Y}_2\text{WO}_9:7\text{ mol\% Er}^{3+}$ phosphors. The device emitted bright green light when operated between a range of 3.4 V to 3.8 V, providing confirmation of the phosphors as possible active media in next-generation optoelectronic and solid-state lighting applications.

CHAPTER 6 : FUTURE SCOPE OF WORK

The encouraging photoluminescent properties of Er^{3+} -doped $\text{Ca}_3\text{Y}_2\text{WO}_9$ (CaYW) phosphors showcased in this work indicate opportunities for future studies. First, energy transfer processes can be enhanced by co-doping with more rare-earth ions (e.g. Yb^{3+} , Tm^{3+}). This may ease concentration quenching and increase quantum yield through co-operative luminescence pathways.

Second, modifying the host matrix through partial chemical substitution of Y^{3+} cation with larger or smaller cations (e.g. Gd^{3+} , La^{3+}) has the potential to stabilize lattice distortions at elevated Er^{3+} contents (>7 mol%) and maintain crystallinity. Third, the morphology of the phosphors can be tuned through more advanced synthesis methods (e.g. sol-gel, hydrothermal) which can provide improvements over the particle agglomeration often experienced during solid-state synthesis, enhancing optical extraction efficiency in LED packaging.

Future studies on thermal stability when exposed to extended operating conditions (greater than 800°C) will be important for high-power LED applications, also studies focused on surface passivation and core-shell structures to minimize thermal degradation. The fact that the material produced broadband NIR emission (~ 1540 nm) is also worth investigating for biomedical imaging and telecommunication applications, which would involve adjusting the host composition for spectral tuning. Moreover, machine learning to optimize the processing sintering parameters and doping profiles could yield a better way to find phosphor compositions w/commercially relevant CCT and CP values.

Ultimately, it would take device integration studies to investigate the performance of prototype w-LEDs, including the CRI value and efficacy metrics at varying drive currents. If the prototype was compared directly on-site with a commercial phosphor such as $\text{YAG}:\text{Ce}^{3+}$, it would more convincingly demonstrate practical feasibility. Life-cycle studies could also examine scaling and the broader environmental profile of mass-producing the phosphors. All of these interdisciplinary approaches will help link lab-scale synthesis work to industrial feasibility for this class of Er^{3+} -activated tungstate phosphors.

CONFERENCE PARTICIPATION CERTIFICATE



Proof of selection in book of abstract

		Noida, Uttar Pradesh-201313	hydroelectric cell	
OT-131	MR. HARIKISHAN SANGANI	Parul University	OT-131 :-Density Functional Theory-Based First-Principles Investigation of the Electronic and Thermoelectric Properties of Sc_2GaRu Heusler Alloy	
OT-132	MS. SWATIJA SAHOO	DELHI TECHNOLOGICAL UNIVERSITY	OT-132 :-Enhanced Photoluminescence Efficiency of Solid State Synthesised Er^{3+} doped phosphor via novel chemical treatment for next generation optoelectronic application	
OT-133	DR. NUTAN RANI	MIRANDA HOUSE, UNIVERSITY OF DELHI, DELHI-110007	OT-133 :-Investigation of Antidiabetic Potential of Biosynthesized ZnO Nanoparticles	
		DEENBANDHU CHHOTU RAM UNIVERSITY OF		

I am happy to share that my abstract has been accepted for the Book of Abstracts of the 3rd International Conference organized by ARSD. This acceptance indicates the credibility and academic and scientific legitimacy and significance of my research, as it has been reviewed and selected by a panel of experts insightful to the topic field as a whole. Having my abstract published as part of this reputable publication not only shows that my research is novel and has potential for impact but also allows me the opportunity to connect with a global audience

of researchers and practitioners. I have no doubt that this is an achievement that shows the quality and significance of my research, as represented in this thesis.

Paper shortlisted in Journal of Electronic Materials(JEMs)

Paper No. Title & : OT-132 Structural and Spectroscopic Insights of Solid-State Synthesised Er³⁺ Doped CaYW Phosphor for Next-Generation Optoelectronic Applications

Dear Prof./Dr./Mr./Ms. Shailesh Narain Sharma and A.S. Rao

Department of Applied Physics, Delhi Technological University

Greetings,

We are pleased to inform you that your paper, submitted to the AFMD 2025 conference, has been shortlisted for potential publication in the Journal of Electronic Materials (JEMs), following the initial screening by the AFMD 2025 Technical Committee.

To proceed, you are requested to submit your manuscript to the JEMs portal by 30th April 2025, following the submission guidelines and using the template provided on the JEMs website.

Paper submitted in Journal of Electronic Materials(JEMs)

JEMS-D-25-00998 -
Submission Notification
to co-author - ★
[EMID:50661b378cb89efe]

Most Important



Journal of E... 30 Apr
to me ▾



Re:
Submission ID: JEMS-D-25-00998
"Structural and Spectroscopic Insights of Solid-State Synthesised Er³⁺ Doped CaYW Phosphor for Next-Generation Optoelectronic Applications"
Full author list: Swatija Sahoo; Bhawna Rajpal; Shailesh Narain Sharma; AS Rao

Dear Ms Sahoo,

We have received the submission entitled: "Structural and Spectroscopic Insights of Solid-State Synthesised Er³⁺ Doped CaYW Phosphor for Next-Generation Optoelectronic Applications" for possible publication

REFERENCES

1. Lin CC, Liu RS (2011) Advances in phosphors for light-emitting diodes. *Journal of Physical Chemistry Letters* 2:1268–1277. https://doi.org/10.1021/JZ2002452/ASSET/IMAGES/MEDIUM/JZ-2011-002452_0009.GIF
2. Kim YH, Viswanath NSM, Unithrattil S, et al (2018) Review—Phosphor Plates for High-Power LED Applications: Challenges and Opportunities toward Perfect Lighting. *ECS Journal of Solid State Science and Technology* 7:R3134–R3147. <https://doi.org/10.1149/2.0181801JSS/XML>
3. Xie RJ, Hirotsaki N, Li Y, Takeda T (2010) Rare-Earth Activated Nitride Phosphors: Synthesis, Luminescence and Applications. *Materials* 2010, Vol 3, Pages 3777-3793 3:3777–3793. <https://doi.org/10.3390/MA3063777>
4. Sekar R, Ravitchandiran A, Angaiah S (2022) Recent Advances and Challenges in Light Conversion Phosphor Materials for Third-Generation Quantum-Dot-Sensitized Photovoltaics. *ACS Omega* 7:35351–35360. https://doi.org/10.1021/ACSOMEGA.2C03736/ASSET/IMAGES/LARGE/AO2C03736_0011.JPEG
5. Zhao M, Xia Z, Huang X, et al (2019) Li substituent tuning of LED phosphors with enhanced efficiency, tunable photoluminescence, and improved thermal stability. *Sci Adv* 5:. https://doi.org/10.1126/SCIADV.AAV0363/SUPPL_FILE/AAV0363_SM.PDF
6. Fang MH, Bao Z, Huang WT, Liu RS (2022) Evolutionary Generation of Phosphor Materials and Their Progress in Future Applications for Light-Emitting Diodes. *Chem Rev* 122:11474–11513. https://doi.org/10.1021/ACS.CHEMREV.1C00952/ASSET/IMAGES/MEDIUM/CR1C00952_0044.GIF
7. Blasse G, Grabmaier BC (1994) A General Introduction to Luminescent Materials. *Luminescent Materials* 1–9. https://doi.org/10.1007/978-3-642-79017-1_1
8. Dorenbos P (2000) The 5d level positions of the trivalent lanthanides in inorganic compounds. *J Lumin* 91:155–176. [https://doi.org/10.1016/S0022-2313\(00\)00229-5](https://doi.org/10.1016/S0022-2313(00)00229-5)
9. (2013) *Molecular Fluorescence: Principles and Applications* [Paperback]. 592
10. (2006) *Instrumentation for Fluorescence Spectroscopy. Principles of Fluorescence Spectroscopy* 27–61. https://doi.org/10.1007/978-0-387-46312-4_2
11. Ronda CR. (2008) *Luminescence : from theory to applications*. 260
12. *Modern Molecular Photochemistry* - Nicholas J. Turro - Google Books. <https://books.google.nl/books?hl=en&lr=&id=KPlz1EEDiXsC&oi=fnd&pg=PA8&dq=Mo>

dern+Molecular+Photochemistry&ots=mXzJvZ43q2&sig=wcbtKIsekdwDmuoXO6TafwThk6s&redir_esc=y#v=onepage&q=Modern%20Molecular%20Photochemistry&f=false.
Accessed 5 Jun 2025

13. El-Sayed MA (1963) Spin—Orbit Coupling and the Radiationless Processes in Nitrogen Heterocyclics. *J Chem Phys* 38:2834–2838. <https://doi.org/10.1063/1.1733610>
14. (2013) *Molecular Fluorescence: Principles and Applications* [Paperback]. 592
15. Pimputkar S, Speck JS, Denbaars SP, Nakamura S (2009) Prospects for LED lighting. *Nat Photonics* 3:180–182. <https://doi.org/10.1038/NPHOTON.2009.32>;KWRD=PHYSICS
16. Schubert EF, Kim JK (2005) Solid-state light sources getting smart. *Science* (1979) 308:1274–1278.
<https://doi.org/10.1126/SCIENCE.1108712>;WEBSITE:WEBSITE:AAAS-SITE;JOURNAL:JOURNAL:SCIENCE;WGROU:STRING:PUBLICATION
17. Edgar A (2017) *Luminescent Materials*. Springer Handbooks 1–1.
https://doi.org/10.1007/978-3-319-48933-9_38
18. Wang Y, Zhu G, Xin S, et al (2015) Recent development in rare earth doped phosphors for white light emitting diodes. *Journal of Rare Earths* 33:1–12. [https://doi.org/10.1016/S1002-0721\(14\)60375-6](https://doi.org/10.1016/S1002-0721(14)60375-6)
19. Wyszecki G, Stiles WS (1982) *Color Science: concepts and methods, quantitative and formulae*. 950
20. (2020) Roy S.Berns, Billmeyer and Saltzman's *Principles of Color Technology*, Fourth edition \$150.00 List Price, \$99.70 on Amazon. 2019. John Wiley & Sons, Inc. 272 pages. ISBN: 978-1-119-3668-3. *Color Res Appl* 45:186. <https://doi.org/10.1002/COL.22445>
21. ETDEWEB: Project Metadata. <https://www.osti.gov/etdeweb/biblio/20123208>. Accessed 5 Jun 2025
22. (2006) *Instrumentation for Fluorescence Spectroscopy*. *Principles of Fluorescence Spectroscopy* 27–61. https://doi.org/10.1007/978-0-387-46312-4_2
23. De Sá GF, Malta OL, De Mello Donegá C, et al (2000) Spectroscopic properties and design of highly luminescent lanthanide coordination complexes. *Coord Chem Rev* 196:165–195. [https://doi.org/10.1016/S0010-8545\(99\)00054-5](https://doi.org/10.1016/S0010-8545(99)00054-5)
24. Dabre KV, Wani JA, Dhoble SJ, et al (2021) Luminescence Properties of Rare Earth–Doped Cubic Double Perovskite Tungstate Ba₂(1–x)(Na,RE)xZnWO₆ (RE = Ce³⁺, Eu³⁺ and Dy³⁺) Phosphors. *physica status solidi (b)* 258:2000442. <https://doi.org/10.1002/PSSB.202000442>

25. Prasad M, Mondal M, Mukhopadhyay L, et al (2021) Photoluminescence investigation in tungstate based materials. *Mater Today Proc* 46:6388–6391. <https://doi.org/10.1016/J.MATPR.2020.06.132>
26. Xiao Q, Zhou Q, Li M (2010) Synthesis and photoluminescence properties of Sm³⁺-doped CaWO₄ nanoparticles. *J Lumin* 130:1092–1094. <https://doi.org/10.1016/J.JLUMIN.2010.02.001>
27. Binnemans K (2009) Lanthanide-based luminescent hybrid materials. *Chem Rev* 109:4283–4374. https://doi.org/10.1021/CR8003983/ASSET/CR8003983.FP.PNG_V03
28. Ricci PC (2020) Assessment of Crystalline Materials for Solid State Lighting Applications: Beyond the Rare Earth Elements. *Crystals* 2020, Vol 10, Page 559 10:559. <https://doi.org/10.3390/CRYST10070559>
29. Edgar A (2017) Luminescent Materials. *Springer Handbooks* 1–1. https://doi.org/10.1007/978-3-319-48933-9_38
30. Xie RJ, Hirosaki N, Li Y, Takeda T (2010) Rare-Earth Activated Nitride Phosphors: Synthesis, Luminescence and Applications. *Materials* 2010, Vol 3, Pages 3777-3793 3:3777–3793. <https://doi.org/10.3390/MA3063777>
31. Gregory NW (1957) Elements of X-Ray Diffraction. *J Am Chem Soc* 79:1773–1774. https://doi.org/10.1021/JA01564A077/ASSET/JA01564A077.FP.PNG_V03
32. Bragg WL (1929) The diffraction of short electromagnetic Waves by a Crystal
33. X-ray Diffraction - Bertram Eugene Warren - Google Books. https://books.google.nl/books?hl=en&lr=&id=wflBhAbEYAsC&oi=fnd&pg=PA1&dq=X-ray+Diffraction&ots=QJOnGEBwsP&sig=Y3hkizB9kbIRDtJhR4CpMD5d-w4&redir_esc=y#v=onepage&q=X-ray%20Diffraction&f=false. Accessed 4 Jun 2025
34. He BB. (2018) Two-dimensional x-ray diffraction. 472
35. Klug HP, Alexander LE (1974) X-Ray Diffraction Procedures: For Polycrystalline and Amorphous Materials, 2nd Edition. xdpf 992
36. (1989) Modern Powder Diffraction. *Modern Powder Diffraction*. <https://doi.org/10.1515/9781501509018/HTML>
37. Scanning Electron Microscopy and X-Ray Microanalysis - Joseph I. Goldstein, Dale E. Newbury, Joseph R. Michael, Nicholas W.M. Ritchie, John Henry J. Scott, David C. Joy - Google Books. https://books.google.nl/books?hl=en&lr=&id=D0I_DwAAQBAJ&oi=fnd&pg=PR5&dq=Scanning+Electron+Microscopy+and+X-ray+Microanalysis&ots=37ON1nHqvg&sig=2VxtwcqFbqBnQLmgkAabroQubdg&redir_esc=y#v=onepage&q=Scanning%20Electron%20Microscopy%20and%20X-ray%20Microanalysis&f=false. Accessed 4 Jun 2025

38. Reimer L (2000) Scanning Electron Microscopy: Physics of Image Formation and Microanalysis, Second Edition. Meas Sci Technol 11:1826. <https://doi.org/10.1088/0957-0233/11/12/703>
39. Williams DB, Carter CB (2009) The Transmission Electron Microscope. Transmission Electron Microscopy 3–22. https://doi.org/10.1007/978-0-387-76501-3_1
40. Infrared Spectroscopy: Fundamentals and Applications - Barbara H. Stuart - Google Books.
https://books.google.nl/books?hl=en&lr=&id=xQVog8RrJKcC&oi=fnd&pg=PR5&dq=Infrared+Spectroscopy:+Fundamentals+and+Applications&ots=LI8ScqcHQi&sig=K10xnt3qzDMTH4QFhzZpFU9N7vU&redir_esc=y#v=onepage&q=Infrared%20Spectroscopy%3A%20Fundamentals%20and%20Applications&f=false. Accessed 4 Jun 2025
41. Fundamentals of Fourier Transform Infrared Spectroscopy - Brian C. Smith - Google Books.
https://books.google.nl/books?hl=en&lr=&id=LR9HkK2cP_0C&oi=fnd&pg=PP1&dq=Fundamentals+of+Fourier+Transform+Infrared+Spectroscopy&ots=iNDgE6YKYz&sig=WQ_ywzsy1DXqt6HzbfDWgTyhKlc&redir_esc=y#v=onepage&q=Fundamentals%20of%20Fourier%20Transform%20Infrared%20Spectroscopy&f=false. Accessed 4 Jun 2025
42. The Infra-red Spectra of Complex Molecules - L. Bellamy - Google Books.
https://books.google.nl/books?hl=en&lr=&id=5KdFBgAAQBAJ&oi=fnd&pg=PA1&dq=The+Infrared+Spectra+of+Complex+Molecules&ots=2V7xHNx1q6&sig=GITXRvjXjYG58Y1YX4Yp5PwfqdM&redir_esc=y#v=onepage&q=The%20Infrared%20Spectra%20of%20Complex%20Molecules&f=false. Accessed 4 Jun 2025
43. Silverstein RW, Bassler GC (1962) Spectrometric identification of organic compounds. J Chem Educ 39:546–553. <https://doi.org/10.1021/ED039P546>
44. Griffiths PR (1983) Fourier Transform Infrared Spectrometry. Science (1979) 222:297–302. <https://doi.org/10.1126/SCIENCE.6623077>
45. Kubelka P, Munk F (1931) An Article on Optics of Paint Layers
46. Tauc J, Grigorovici R, Vancu A (1966) Optical Properties and Electronic Structure of Amorphous Germanium. physica status solidi (b) 15:627–637.
<https://doi.org/10.1002/PSSB.19660150224;SUBPAGE:STRING:ABSTRACT;WEBSITE:WEBSITE:PERICLES;JOURNAL:JOURNAL:15213951;REQUESTEDJOURNAL:JOURNAL:15213951;WGROU:STRING:PUBLICATION>
47. Landi S, Segundo IR, Freitas E, et al (2022) Use and misuse of the Kubelka-Munk function to obtain the band gap energy from diffuse reflectance measurements. Solid State Commun 341:114573. <https://doi.org/10.1016/J.SSC.2021.114573>
48. Optical Processes in Semiconductors - Jacques I. Pankove - Google Books.
<https://books.google.nl/books?hl=en&lr=&id=HHM9Vo0DYZAC&oi=fnd&pg=PA1&dq=>

Optical+Processes+in+Semiconductors&ots=vA00N0CmDi&sig=3sEJKmGgDpHYYOjV
Lt_NEIyM88U&redir_esc=y#v=onepage&q=Optical%20Processes%20in%20Semiconduc
tors&f=false. Accessed 4 Jun 2025

49. Elliott SR (2006) Atomic dynamics. The physics and chemistry of solids 209–288
50. Adachi S (2021) Review—Photoluminescence Properties of Cr³⁺-Activated Oxide Phosphors. ECS Journal of Solid State Science and Technology 10:026001. <https://doi.org/10.1149/2162-8777/ABDC01>
51. Li Q, Anpo M, You J, et al (2023) Photoluminescence (PL) Spectroscopy. Springer Handbooks 295–321. https://doi.org/10.1007/978-3-031-07125-6_14
52. Xu J, Zhu S, Liao C, et al (2024) Upconversion luminescence and thermosensitive properties of NaGd(PO₃)₄:Yb³⁺/Er³⁺. Heliyon 10:. <https://doi.org/10.1016/j.heliyon.2024.e39951>
53. Optical Properties And Spectroscopy Of Nanomaterials - Jin Zhong Zhang - Google Books. https://books.google.nl/books?hl=en&lr=&id=AfLFCgAAQBAJ&oi=fnd&pg=PR7&dq=Principles+of+photoluminescence+spectroscopy+and+applications+to+nanomaterials&ots=WXXkuu1DYD5&sig=r5Ax8bGFuOOX06w5yuU_cwI9Ktc&redir_esc=y#v=onepage&q=Principles%20of%20photoluminescence%20spectroscopy%20and%20applications%20to%20nanomaterials&f=false. Accessed 4 Jun 2025
54. Deshpande SS (2001) Principles and applications of luminescence spectroscopy. Crit Rev Food Sci Nutr 41:155–224. <https://doi.org/10.1080/20014091091797;JOURNAL:JOURNAL:BFSN18;WGROU:STRING:PUBLICATION>
55. Ryba-Romanowski W, Lisiecki R, Rzepka A, et al (2009) Luminescence and excitation energy transfer in rare earth-doped Y₄Al₂O₉ nanocrystals. Opt Mater (Amst) 31:1155–1162. <https://doi.org/10.1016/J.OPTMAT.2008.12.006>
56. Fan N, Du Q, Guo R, et al (2023) Sol-Gel Synthesis and Photoluminescence Properties of a Far-Red Emitting Phosphor BaLaMgTaO₆:Mn⁴⁺ for Plant Growth LEDs. Materials 16:4029. <https://doi.org/10.3390/MA16114029/S1>
57. Yu Y, McCluskey MD (2022) Classification of Semiconductors Using Photoluminescence Spectroscopy and Machine Learning. Appl Spectrosc 76:228–234. https://doi.org/10.1177/00037028211031618/SUPPL_FILE/SJ-PDF-1-ASP-10.1177_00037028211031618.PDF
58. Mayavan A (2023) Comprehensive Review on Downconversion/Downshifting Silicate-Based Phosphors for Solar Cell Applications. ACS Omega. https://doi.org/10.1021/ACSOMEGA.3C08806/ASSET/IMAGES/LARGE/AO3C08806_0008.JPEG

59. Szmazinski H, Lakowicz JR (1995) Fluorescence lifetime-based sensing and imaging. *Sens Actuators B Chem* 29:16–24. [https://doi.org/10.1016/0925-4005\(95\)01658-9](https://doi.org/10.1016/0925-4005(95)01658-9)
60. Chen MC (2019) Lanthanide Energy Transfer Donors on Nanoparticles Surfaces : From Fundamental Mechanisms to Multiplexed Biosensing. <https://doi.org/10.34894/VQ1DJA>
61. Ma L, Yang F, Zheng J (2014) Application of fluorescence resonance energy transfer in protein studies. *J Mol Struct* 1077:87–100. <https://doi.org/10.1016/J.MOLSTRUC.2013.12.071>
62. Gopal R, Manam J (2022) SrWO₄: Er³⁺; an efficient green phosphor for LED and optical thermometry applications. *Journal of Materials Science: Materials in Electronics* 33:21746–21761. <https://doi.org/10.1007/S10854-022-08964-6/METRICS>
63. Kumar A, Singh DK, Manam J (2019) Structural and optical properties of highly thermally active Gd₂Zr₂O₇:Dy³⁺ phosphors for lighting applications. *Journal of Materials Science: Materials in Electronics* 30:2360–2372. <https://doi.org/10.1007/S10854-018-0509-8/METRICS>
64. Gao H, Yu C, Wang Y, et al (2022) A novel photoluminescence phenomenon in a SrMoO₄/SrWO₄ micro/nano heterojunction phosphors obtained by the polyacrylamide gel method combined with low temperature calcination technology. *J Lumin* 243:118660. <https://doi.org/10.1016/J.JLUMIN.2021.118660>
65. Wang S, Gao H, Wang Y, et al (2020) Effect of the Sintering Process on the Structure, Colorimetric, Optical and Photoluminescence Properties of SrWO₄ Phosphor Powders. *J Electron Mater* 49:2450–2462. <https://doi.org/10.1007/S11664-020-07941-1/METRICS>
66. Pandey A, Rai VK, Kumar V, et al (2015) Upconversion based temperature sensing ability of Er³⁺–Yb³⁺-codoped SrWO₄: An optical heating phosphor. *Sens Actuators B Chem* 209:352–358. <https://doi.org/10.1016/J.SNB.2014.11.126>
67. Maheshwary, Singh BP, Singh RA (2009) Effect of annealing on the structural, optical and emissive properties of SrWO₄:Ln(3+) (Dy(3+), Eu(3+) and Sm(3+)) nanoparticles. *Spectrochim Acta A Mol Biomol Spectrosc* 152:199–207. <https://doi.org/10.1016/J.SAA.2015.07.074>
68. Kumar A, Singh DK, Manam J (2019) Structural and optical properties of highly thermally active Gd₂Zr₂O₇:Dy³⁺ phosphors for lighting applications. *Journal of Materials Science: Materials in Electronics* 30:2360–2372. <https://doi.org/10.1007/S10854-018-0509-8/METRICS>
69. Kumar Singh D, Mondal K, Manam J (2017) Improved photoluminescence, thermal stability and temperature sensing performances of K⁺ incorporated perovskite BaTiO₃:Eu³⁺ red emitting phosphors. *Ceram Int* 43:13602–13611. <https://doi.org/10.1016/J.CERAMINT.2017.07.069>

70. Bairy R, Jayarama A, Kulkarni SD, et al (2019) Role of Zn in tuning the band gap, surface morphology, photoluminescence and optical nonlinearities of CdO nanostructures for photonic device applications. *Mater Res Express* 6:096447. <https://doi.org/10.1088/2053-1591/AB3329>
71. Dwivedi A, Roy A, Rai SB (2023) Photoluminescence behavior of rare earth doped self-activated phosphors (i.e. niobate and vanadate) and their applications. *RSC Adv* 13:16260–16271. <https://doi.org/10.1039/D3RA00629H>
72. Zhang H, Zhang H (2022) Special Issue: Rare earth luminescent materials. *Light: Science & Applications* 2022 11:1 11:1–3. <https://doi.org/10.1038/s41377-022-00956-9>
73. Gupta P, Sahni M, Chauhan S (2021) Enhanced photoluminescence properties of rare earth elements doped Y_{0.50}Gd_{0.50}BO₃ phosphor and its application in red and green LEDs. *Optik (Stuttg)* 240:166810. <https://doi.org/10.1016/J.IJLEO.2021.166810>
74. Chen Z, Zhu H, Qian J, et al (2023) Rare Earth Ion Doped Luminescent Materials: A Review of Up/Down Conversion Luminescent Mechanism, Synthesis, and Anti-Counterfeiting Application. *Photonics* 2023, Vol 10, Page 1014 10:1014. <https://doi.org/10.3390/PHOTONICS10091014>
75. Yi SS, Jung JY (2022) Up-conversion luminescence properties with temperature change of strontium tungstate phosphors. *RSC Adv* 12:24752–24759. <https://doi.org/10.1039/D2RA04705E>
76. Kumar A, Manam J (2020) Optical thermometry using up and down conversion photoluminescence mechanism in Y₂Zr₂O₇: Er³⁺ phosphors with excellent sensing sensitivity. *J Alloys Compd* 829:154610. <https://doi.org/10.1016/J.JALLCOM.2020.154610>
77. Kumar A, Manam J (2019) Color tunable emission and temperature dependent photoluminescence properties of Eu³⁺ co-doped Gd₂Zr₂O₇:Dy³⁺ phosphors. *Opt Mater (Amst)* 96:109373. <https://doi.org/10.1016/J.OPTMAT.2019.109373>
78. Kaur S, Rao AS, Jayasimhadri M, et al (2019) Synthesis optimization, photoluminescence and thermoluminescence studies of Eu³⁺ doped calcium aluminozincate phosphor. *J Alloys Compd* 802:129–138. <https://doi.org/10.1016/J.JALLCOM.2019.06.169>
79. Kaczorowska N, Szczeszak A, Lis S (2018) Synthesis and tunable emission studies of new up-converting Ba₂GdV₃O₁₁ nanopowders doped with Yb³⁺/Ln³⁺ (Ln³⁺ = Er³⁺, Ho³⁺, Tm³⁺). *J Lumin* 200:59–65. <https://doi.org/10.1016/J.JLUMIN.2018.03.085>
80. Zambare PZ, Girase KD, R Murthy K V, et al (2013) ADVANCED MATERIALS Letters Thermal analysis and luminescent properties of Sr₂CeO₄ blue phosphor. *Research Article Adv Mat Lett* 2013:577–581. <https://doi.org/10.5185/amlett.2012.11457>

81. Vishwakarma AK, Jha K, Jayasimhadri M, et al (2015) Red light emitting BaNb₂O₆:Eu³⁺ phosphor for solid state lighting applications. *J Alloys Compd* 622:97–101. <https://doi.org/10.1016/J.JALLCOM.2014.10.016>
82. Rambabu U, Munirathnam NR, Prakash TL, Buddhudu S (2003) Emission spectra of LnPO₄:RE³⁺ (Ln=La, Gd; RE=Eu, Tb and Ce) powder phosphors. *Mater Chem Phys* 78:160–169. [https://doi.org/10.1016/S0254-0584\(02\)00294-8](https://doi.org/10.1016/S0254-0584(02)00294-8)
83. Maheshwari K, Rao AS (2023) Down-shifting photoluminescent properties of Tb³⁺ doped phosphate glasses for intense green-emitting devices applications. *Opt Mater (Amst)* 137:113533. <https://doi.org/10.1016/J.OPTMAT.2023.113533>
84. Kumari S, Rao AS, Sinha RK (2023) Structural and photoluminescence properties of Sm³⁺ ions doped strontium yttrium tungstate phosphors for reddish-orange photonic device applications. *Mater Res Bull* 167:112419. <https://doi.org/10.1016/J.MATERRESBULL.2023.112419>

SWATIJA SAHOO THESIS 2025 ABSTRACT.docx

PLAGIARISM REPORT

 Delhi Technological University

Document Details

Submission ID**trn:oid:::27535:99358572****Submission Date****Jun 4, 2025, 10:55 PM GMT+5:30****Download Date****Jun 4, 2025, 10:56 PM GMT+5:30****File Name****SWATIJA SAHOO THESIS 2025 ABSTRACT.docx****File Size****2.1 MB**

34 Pages

9,598 Words

54,206 Characters





6% Overall Similarity

The combined total of all matches, including overlapping sources, for each database.




Filtered from the Report

- Bibliography
- Small Matches (less than 10 words)

Match Groups

-  **46** Not Cited or Quoted 6%
Matches with neither in-text citation nor quotation marks
-  **0** Missing Quotations 0%
Matches that are still very similar to source material
-  **0** Missing Citation 0%
Matches that have quotation marks, but no in-text citation
-  **0** Cited and Quoted 0%
Matches with in-text citation present, but no quotation marks

Top Sources

- 3%  Internet sources
- 3%  Publications
- 3%  Submitted works (Student Papers)

Integrity Flags

0 Integrity Flags for Review

No suspicious text manipulations found.

Our system's algorithms look deeply at a document for any inconsistencies that would set it apart from a normal submission. If we notice something strange, we flag it for you to review.

A Flag is not necessarily an indicator of a problem. However, we'd recommend you focus your attention there for further review.

Match Groups

- 46** Not Cited or Quoted 6%
Matches with neither in-text citation nor quotation marks
- 0** Missing Quotations 0%
Matches that are still very similar to source material
- 0** Missing Citation 0%
Matches that have quotation marks, but no in-text citation
- 0** Cited and Quoted 0%
Matches with in-text citation present, but no quotation marks

Top Sources

- 3% Internet sources
- 3% Publications
- 3% Submitted works (Student Papers)

Top Sources

The sources with the highest number of matches within the submission. Overlapping sources will not be displayed.

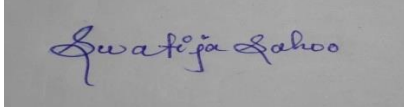
- Publication
Jatin Parashar, Gaurank Yadav, Seema, Anu, Aman Prasad, A. S. Rao. "Energy Tra... <1%
- Publication
Ravi Shrivastava, Jagjeet Kaur, Vikas Dubey. "White Light Emission by Dy3+ Doped... <1%
- Publication
F. Wang, X. Liu. "Rare-Earth Doped Upconversion Nanophosphors", Elsevier BV, 20... <1%
- Internet
worldwidescience.org <1%
- Publication
M.D. Mehare, Chaitali M. Mehare, H.C. Swart, S.J. Dhoble. "Recent Development in... <1%
- Publication
Mihail Nazarov, Do Young Noh. "New Generation of Europium- and Terbium-Activ... <1%
- Submitted works
Nottingham Trent University on 2024-08-21 <1%
- Submitted works
SASTRA University on 2017-10-16 <1%
- Submitted works
University of Keele on 2025-05-09 <1%
- Publication
Ishwar Prasad Sahu, D. P. Bisen, N. Brahme, Raunak Kumar Tamrakar. "Generatio... <1%

11	Submitted works	Cranfield University on 2012-08-30	<1%
12	Internet	pubs.rsc.org	<1%
13	Internet	www.jmaterenvironsci.com	<1%
14	Internet	studentsrepo.um.edu.my	<1%
15	Internet	www.bville.org	<1%
16	Submitted works	Indian Institute of Management, Indore on 2017-06-15	<1%
17	Internet	dalspace.library.dal.ca	<1%
18	Internet	ijariie.com	<1%
19	Submitted works	Higher Education Commission Pakistan on 2018-10-31	<1%
20	Submitted works	Indian Institute of Technology on 2020-12-21	<1%
21	Submitted works	Thapar University, Patiala on 2019-07-06	<1%
22	Submitted works	The Hong Kong Polytechnic University on 2013-08-26	<1%
23	Internet	dr.ntu.edu.sg	<1%
24	Internet	etd.lib.nctu.edu.tw	<1%

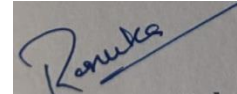
25	Submitted works	University College London on 2015-07-05	<1%
26	Publication	Yu, J.. "Photoluminescence of double-color-emitting phosphor $\text{Ca}^{2+}_5(\text{PO}_4)_3\text{Cl}:\text{E}...$	<1%
27	Internet	epgp.inflibnet.ac.in	<1%
28	Internet	www.mdpi.com	<1%
29	Publication	Hayder Salah Naeem, Iskandar Shahrin Mustafa, N.N. Yusof, Hammam Abdurab...	<1%
30	Submitted works	IIT Delhi on 2014-04-30	<1%
31	Submitted works	Jawaharlal Nehru Technological University Anantapur on 2014-07-08	<1%
32	Publication	S.K. Sharma, S. Som, R. Jain, A.K. Kunti. "Spectral and CIE parameters of red emitti...	<1%
33	Submitted works	The Energy and Resources Institute on 2013-02-20	<1%
34	Publication	Willem J. van den Hoek, Gerardus M. J. F. Luijckx, Josephus J. Degroot. "Lamps", Wil...	<1%

35	Publication	Zhao Ming, Pan Xiangqing, Yimin Wang. "Preparation and Characterization of Pol...	<1%
36	Internet	ebin.pub	<1%
37	Internet	journals.iucr.org	<1%

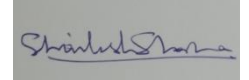
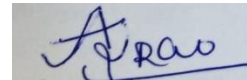
SIGNATURE OF THE STUDENT



SIGNATURE OF THE SUPERVISOR



SIGNATURES OF CO-SUPERVISORS



Proof of Scopus/SCI/SCIE index

Filters [Clear All](#)

Web of Science Coverage ^

Core Collection

- ☒ Science Citation Index Expanded (SCIE)
- ☐ Social Sciences Citation Index (SSCI)
- ☐ Arts & Humanities Citation Index (AHCI)
- ☐ Emerging Sources Citation Index (ESCI)

Current Contents

- ☐ Agriculture, Biology & Environmental Sciences
- ☐ Arts & Humanities

SCIENCE CITATION INDEX EXPANDED (SCIE) x

Search Results

Found 1,050 results (Page 1) [Share These Results](#)

Exact Match Found

JOURNAL OF ELECTRONIC MATERIALS

Publisher: **SPRINGER** ONE NEW YORK PLAZA, SUITE 4600 , NEW YORK, United States, NY, 10004

ISSN / eISSN: 0361-5235 / 1543-186X

Web of Science Core Collection: **Science Citation Index Expanded**

Additional Web of Science Indexes: Current Contents Electronics & Telecommunications Collection | Current Contents Physical, Chemical & Earth Sciences | Essential Science Indicators

[Share This Journal](#) [View profile page](#)

Journal information

Electronic ISSN	Print ISSN
1543-186X	0361-5235

Abstracted and indexed in

Astrophysics Data System (ADS)

BFI List

Baidu

CLOCKSS

CNKI

CNPIEC

Chemical Abstracts Service (CAS)

Chimica

Current Contents/Electronics & Telecommunications Collection

Current Contents/Physical, Chemical and Earth Sciences

Dimensions

EBSCO

EI Compendex

Google Scholar

INSPEC

Japanese Science and Technology Agency (JST)

Naver

OCLC WorldCat Discovery Service

Portico

ProQuest

SCImago

SCOPUS

Science Citation Index Expanded (SCIE)

Semantic Scholar

TD Net Discovery Service

Wanfang

<https://link.springer.com/journal/11664>